samples, suggesting that only the Ser585 survival "arm" of the βc phospho-binary switch is subject to deregulation in AML.

Thus, we observe a clear distinction between the GM-CSF receptor Ser585 phosphorylation pathway (which is constitutive) and receptor tyrosine phosphorylation pathways (which remain cytokine dependent) in primary AML samples. Others have examined the prevalence of cytokine receptor tyrosine signaling pathways in AML samples. For example, constitutive STAT, p38, and ERK activation/phosphorylation have been observed in 25% to 70% of AML samples with many phospho-protein networks remaining cytokine dependent with low basal signals.[29-31] Collectively, these studies show that, although cytokine signaling pathways are frequently subject to deregulation in AML, the extent of this deregulation varies. Given this variation, the prevalence of constitutive Ser585 phosphorylation observed in our studies (20 of 23) is particularly striking and represents a common theme observed across a spectrum of patients with AML.

The deregulation of the normal cellular machinery that controls the axis between cell survival and death is proposed to be a key event in cellular transformation. However, to our knowledge, the specific comparison of cell survival-only expression profiles between nontransformed and transformed cells has not been reported. Our results show that *BCL2*, *VRK1*, *POLR2C*, *CDK8*, *FNDC3*, and *PTPRS* were identified as being in the Ser585/PI3-kinase gene network and were highly expressed in both $CD34^+$ cells derived from both healthy donors and AML patient samples (Figure 4). These results would suggest that the normal cell survival pathways that operate in nontransformed $CD34^+$ cells also operate in AML blasts. The role of any of these genes in the pathogenesis of AML remains to be determined; however, *BCL2* is a prosurvival gene that has been shown to cooperate with *c-MYC* in promoting lymphoma in animal models.[21] Both *POLR2C* and *CDK8* are part of the mediator complex,[32] and *CDK8* has recently been shown to act as an oncogene in colon cancer.[33,34] Importantly, MacKeigan et al[22] identified *CDK8* and *PTPRS* in an siRNA screen for kinases and phosphatases regulating cell survival, suggesting that deregulation of these genes may promote autonomous cell survival in AML.

Another gene identified as being part of the Ser585/PI3-kinase survival pathway was *OPN*. We have analyzed *OPN* expression in 130 AML samples with diverse cytogenetic abnormalities and found a broad range of expression across all FAB subgroups (Figure 7B). Univariate analysis of OS in all patients treated with induction chemotherapy at our institution (n = 52) showed that high *OPN* expression was associated with poor OS (median, 225 days) compared with low *OPN* (median, 552 days; Figure 7C; $P = .02$), although there was no significance on multivariate analysis. However, multivariate analysis of an expanded cohort of 60 normal-karyotype AMLs from RAH and Kumamoto indicated that *OPN* expression was an independent prognostic indicator of OS (HR, 2.23; 95% CI, 1.23-4.03; Figure 7E; Table 3; $P = .01$) and did not correlate with *FLT3* or *NPM1* mutation status in these patients. Normal cytogenetic AML is the largest clinical subgroup in adult AML (50%-60%) and remains a major clinical challenge in terms of risk stratification, timing of allogeneic transplantation, and lack of efficacious targeted therapy. Only a few prognostic indicators such as *FLT3*, *NPM1*, and *CEBPα* are currently available. In addition to these markers, our study identifies *OPN* as a new prognostic indicator for OS in normal karyotype AML that may have utility in patient stratification and treatment selection. Expanded studies of *OPN* expression in multicenter trials in a range of AML subgroups are warranted.

In addition to acting as a prognostic factor, our results further indicate that high *OPN* expression may play a functional role in promoting deregulated cell survival in AML. Targeting *OPN* expression by siRNA in either AML blasts or LSPCs results in loss of cell viability (Figure 6) and therefore probably represents a key survival factor in leukemic stem cells. The precise mechanistic details by which *OPN* contributes to leukemogenesis remains unclear; however, studies in mice lacking *OPN* suggest that it promotes stem cell quiescence by inhibiting proliferation.[17] Others have shown that OPN can act as a survival factor for activated T cells independently of their proliferation, leading to exacerbation of multiple sclerosis in animal models.[23] Note that other studies using microarray screens of AML patient samples did not identify *OPN* overexpression as a prognostic indicator.[35] However, microarray analysis is known to underestimate expression differences compared with quantitative RT-PCR. Nevertheless, high OPN protein levels in the plasma and blood of patients with a range of solid tumors as well as AML have been reported, and in some cases high OPN levels have been linked to poor prognosis.[36-38] Thus, deregulated expression of *OPN* may play an important pathogenic role by deregulating survival programs in diverse cancers beyond leukemia.

OPN is a secreted phosphoprotein that acts as a cytokine and chemoattractant to regulate pleiotropic responses in diverse cell types, including hemopoietic cells.[39] In part, the pleiotropic activities of *OPN* are probably due to its ability to bind different cell surface receptors that include CD44 and specific integrins in the αβ family.[39] *OPN* expression in the bone marrow is tightly regulated and expressed at the endosteal interface of bone and hemopoietic tissue where it is secreted by osteoblasts.[39] Interestingly, Lin et al[24] have shown that IL-3 stimulation of Ba/F3 cells induces *OPN* expression, which in turn promotes hemopoietic cell survival via the CD44 receptor. It is not yet clear which receptor system *OPN* uses to promote cell survival in AML blasts and LSPCs in our studies. However, mAbs to CD44 not only reduce disease burden in animal models of AML but also abrogate AML in mice that serially received a transplant, indicating that the therapeutic response was most likely because of the targeting of CD44 in LSPCs.[40] Similarly, a mAb to CD44 also blocks the homing and engraftment of chronic myeloid leukemia (CML) cells in murine models.[41] Given that *OPN*-null mice are viable and fertile and have a mild phenotype,[17] it is possible that targeting *OPN* may represent an important avenue for the development of therapeutics that block deregulated survival in leukemia.

Our identification of a phosphoserine pathway that is deregulated in AML has important implications for the treatment of leukemia. The early picture emerging from clinical trials that used tyrosine kinase inhibitors (TKIs) for the treatment of cancer is that they are often highly effective in providing an initial response by preventing cell proliferation, but they are less effective in blocking the survival of quiescent LSPCs. Even with the remarkable success of imatinib in treating CML, minimal residual disease is clearly detectable in more than 90% of patients in remission because of the survival of a population of CML progenitors that are refractory to TKI therapy.[42-44] Furthermore, the results from clinical trials that used FLT3 TKIs indicate that, although they are very effective at blocking FLT3 tyrosine phosphorylation in patient samples and are able to block FLT3-mediated proliferation, they show modest anticancer activity that provides partial remissions of short duration.[45-47] Thus, targeting phosphotyrosine-independent cell survival-only programs in AML such as *OPN* may provide a complementary

therapeutic approach to eradicate the quiescent long-term surviving LSPCs.

Acknowledgments

We thank Dr Andrew Zannettino from the Department of Hematology, Center for Cancer Biology, for supplying reagents; Nancy Briggs and Tom Sullivan from the School of Medicine, University of Adelaide, for statistical support; and Kate Harrison and Monika Kutyna (Department of Hematology, Center for Cancer Biology) for patient mutational studies.

This work was supported by grants from the National Health and Medical Research Council of Australia and the Cancer Council of South Australia. M.A.G. was supported as a Peter Nelson Leukemia Research Fellow. D.T. is a recipient of a Haemtology and Oncology Targeted Therapy (HOTT) Fellowship administered by the Hematology Society of Australia and New Zealand (Clinical Oncology Society of Australia [COSA], Roche, Medical Oncology Group of Australia [MOGA]).

Authorship

Contribution: J.A.P., M.A.G. designed and performed research, analyzed and interpreted data, and wrote the paper; D.T. performed research, analyzed and interpreted data, and wrote the paper; E.F.B., B.J.M., A.B., and B.J. performed research; C.H.K., A.T., and T.P.S. performed statistical analysis; L.B.T., I.D.L., K.H., and N.A. provided vital AML patient samples; G.J.G., R.J.D., and A.F.L. analyzed and interpreted data; and M.O., D.N.H., and S.K.N. performed research and analyzed and interpreted data.

Conflict-of-interest disclosure: A.F.L. receives honoraria from CSL Limited, Australia. The remaining authors declare no competing financial interests.

Correspondence: Mark A. Guthridge, Cell Growth and Differentiation Laboratory, Division of Human Immunology, Centre for Cancer Biology, SA Pathology, Frome Rd, Adelaide, SA, Australia 5000; e-mail: mark.guthridge@imvs.sa.gov.au.

References

1. Evan GI, Vousden KH. Proliferation, cell cycle and apoptosis in cancer. *Nature.* 2001;411(6835):342-348.
2. Begley CG, Lopez AF, Nicola NA, et al. Purified colony-stimulating factors enhance the survival of human neutrophils and eosinophils in vitro: a rapid and sensitive microassay for colony-stimulating factors. *Blood.* 1986;68(1):162-166.
3. Williams GT, Smith CA, Spooncer E, Dexter TM, Taylor DR. Haemopoietic colony stimulating factors promote cell survival by suppressing apoptosis. *Nature.* 1990;343(6253):76-79.
4. Pelengaris S, Khan M, Evan G. c-MYC: more than just a matter of life and death. *Nat Rev Cancer.* 2002;2(10):764-776.
5. Reilly JT. Receptor tyrosine kinases in normal and malignant haematopoiesis. *Blood Rev.* 2003;17(4):241-248.
6. D'Andrea RJ, Harrison-Findik D, Butcher CM, et al. Dysregulated hematopoiesis and a progressive neurological disorder induced by expression of an activated form of the human common beta chain in transgenic mice. *J Clin Invest.* 1998;102(11):1951-1960.
7. Bollag G, Clapp DW, Shih S, et al. Loss of NF1 results in activation of the Ras signaling pathway and leads to aberrant growth in haematopoietic cells. *Nat Genet.* 1996;12(2):144-148.
8. Helgason CD, Damen JE, Rosten P, et al. Targeted disruption of SHIP leads to hemopoietic perturbations, lung pathology, and a shortened life span. *Genes Dev.* 1998;12(11):1610-1620.
9. Vivanco I, Sawyers CL. The phosphatidylinositol 3-Kinase AKT pathway in human cancer. *Nat Rev Cancer.* 2002;2(7):489-501.
10. Guthridge MA, Stomski FC, Barry EF, et al. Site-specific serine phosphorylation of the IL-3 receptor is required for hemopoietic cell survival. *Mol Cell.* 2000;6(1):99-108.
11. Guthridge MA, Barry EF, Felquer FA, et al. The phosphoserine-585-dependent pathway of the GM-CSF/IL-3/IL-5 receptors mediates hematopoietic cell survival through activation of NF-kappaB and induction of bcl-2. *Blood.* 2004;103(3):820-827.
12. Guthridge MA, Powell JA, Barry EF, et al. Growth factor pleiotropy is controlled by a receptor Tyr/Ser motif that acts as a binary switch. *EMBO J.* 2006;25(3):479-489.
13. Grimwade D, Walker H, Oliver F, et al. The importance of diagnostic cytogenetics on outcome in AML: analysis of 1612 patients entered into the MRC AML 10 trial. The Medical Research Council Adult and Children's Leukaemia Working Parties. *Blood.* 1998;92(7):2322-2333.
14. Bradstock KF, Matthews JP, Lowenthal RM, et al. A randomized trial of high-versus conventional-dose cytarabine in consolidation chemotherapy for adult de novo acute myeloid leukemia in first remission after induction therapy containing high-dose cytarabine. *Blood.* 2005;105(2):481-488.
15. Ohno R, Kobayashi T, Tanimoto M, et al. Randomized study of individualized induction therapy with or without vincristine, and of maintenance-intensification therapy between 4 or 12 courses in adult acute myeloid leukemia. AML-87 Study of the Japan Adult Leukemia Study Group. *Cancer.* 1993;71(12):3888-3895.
16. Miyawaki S, Sakamaki H, Ohtake S, et al. A randomized, postremission comparison of four courses of standard-dose consolidation therapy without maintenance therapy versus three courses of standard-dose consolidation with maintenance therapy in adults with acute myeloid leukemia: the Japan Adult Leukemia Study Group AML 97 Study. *Cancer.* 2005;104(12):2726-2734.
17. Nilsson SK, Johnston HM, Whitty GA, et al. Osteopontin, a key component of the hematopoietic stem cell niche and regulator of primitive hematopoietic progenitor cells. *Blood.* 2005;106(4):1232-1239.
18. Christensen B, Nielsen MS, Haselmann KF, Petersen TE, Sorensen ES. Post-translationally modified residues of native human osteopontin are located in clusters: identification of 36 phosphorylation and five O-glycosylation sites and their biological implications. *Biochem J.* 2005;390(Pt 1):285-292.
19. Lamb J, Crawford ED, Peck D, et al. The Connectivity Map: using gene-expression signatures to connect small molecules, genes, and disease. *Science.* 2006;313(5795):1929-1935.
20. Tamburini J, Elie C, Bardet V, et al. Constitutive phosphoinositide 3-kinase/Akt activation represents a favorable prognostic factor in de novo acute myelogenous leukemia patients. *Blood.* 2007;110(3):1025-1028.
21. Vaux DL, Cory S, Adams JM. Bcl-2 gene promotes haemopoietic cell survival and cooperates with c-myc to immortalize pre-B cells. *Nature.* 1988;335(6189):440-442.
22. MacKeigan JP, Murphy LO, Blenis J. Sensitized RNAi screen of human kinases and phosphatases identifies new regulators of apoptosis and chemoresistance. *Nat Cell Biol.* 2005;7(6):591-600.
23. Hur EM, Youssef S, Haws ME, et al. Osteopontin-induced relapse and progression of autoimmune brain disease through enhanced survival of activated T cells. *Nat Immunol.* 2007;8(1):74-83.
24. Lin YH, Huang CJ, Chao JR, et al. Coupling of osteopontin and its cell surface receptor CD44 to the cell survival response elicited by interleukin-3 or granulocyte-macrophage colony-stimulating factor. *Mol Cell Biol.* 2000;20(8):2734-2742.
25. Dinndorf PA, Andrews RG, Benjamin D, et al. Expression of normal myeloid-associated antigens by acute leukemia cells. *Blood.* 1986;67(4):1048-1053.
26. Lapidot T, Sirard C, Vormoor J, et al. A cell initiating human acute myeloid leukaemia after transplantation into SCID mice. *Nature.* 1994;367(6464):645-648.
27. Jordan CT, Upchurch D, Szilvassy SJ, et al. The interleukin-3 receptor alpha chain is a unique marker for human acute myelogenous leukemia stem cells. *Leukemia.* 2000;14(10):1777-1784.
28. Hanahan D, Weinberg RA. The hallmarks of cancer. *Cell.* 2000;100(1):57-70.
29. Kim SC, Hahn JS, Min YH, et al. Constitutive activation of extracellular signal-regulated kinase in human acute leukemias: combined role of activation of MEK, hyperexpression of extracellular signal-regulated kinase, and downregulation of a phosphatase, PAC1. *Blood.* 1999;93(11):3893-3899.
30. Gouilleux-Gruart V, Gouilleux F, Desaint C, et al. STAT-related transcription factors are constitutively activated in peripheral blood cells from acute leukemia patients. *Blood.* 1996;87(5):1692-1697.
31. Irish JM, Hovland R, Krutzik PO, et al. Single cell profiling of potentiated phospho-protein networks in cancer cells. *Cell.* 2004;118(2):217-228.
32. Conaway RC, Sato S, Tomomori-Sato C, Yao T, Conaway JW. The mammalian Mediator complex and its role in transcriptional regulation. *Trends Biochem Sci.* 2005;30(5):250-255.
33. Morris EJ, Ji JY, Yang F, et al. E2F1 represses beta-catenin transcription and is antagonized by both pRB and CDK8. *Nature.* 2008;455(7212):552-556.
34. Firestein R, Bass AJ, Kim SY, et al. CDK8 is a colorectal cancer oncogene that regulates beta-catenin activity. *Nature.* 2008;455(7212):547-551.
35. Valk PJ, Verhaak RG, Beijen MA, et al. Prognostically useful gene-expression profiles in acute myeloid leukemia. *N Engl J Med.* 2004;350(16):1617-1628.

36. Rittling SR, Chambers AF. Role of osteopontin in tumour progression. *Br J Cancer.* 2004;90(10): 1877-1881.

37. Lee CY, Tien HF, Hou HA, Chou WC, Lin LI. Marrow osteopontin level as a prognostic factor in acute myeloid leukaemia. *Br J Haematol.* 2008; 141(5):736-739.

38. Ramankulov A, Lein M, Kristiansen G, et al. Elevated plasma osteopontin as marker for distant metastases and poor survival in patients with renal cell carcinoma. *J Cancer Res Clin Oncol.* 2007;133(9):643-652.

39. Haylock DN, Nilsson SK. Osteopontin: a bridge between bone and blood. *Br J Haematol.* 2006; 134(5):467-474.

40. Jin L, Hope KJ, Zhai Q, Smadja-Joffe F, Dick JE. Targeting of CD44 eradicates human acute myeloid leukemic stem cells. *Nat Med.* 2006;12(10): 1167-1174.

41. Krause DS, Lazarides K, von Andrian UH, Van Etten RA. Requirement for CD44 in homing and engraftment of BCR-ABL-expressing leukemic stem cells. *Nat Med.* 2006;12(10):1175-1180.

42. Hughes TP, Kaeda J, Branford S, et al. Frequency of major molecular responses to imatinib or interferon alfa plus cytarabine in newly diagnosed chronic myeloid leukemia. *N Engl J Med.* 2003;349(15):1423-1432.

43. Bhatia R, Holtz M, Niu N, et al. Persistence of malignant hematopoietic progenitors in chronic myelogenous leukemia patients in complete cytogenetic remission following imatinib mesylate treatment. *Blood.* 2003;101(12):4701-4707.

44. Copland M, Hamilton A, Elrick LJ, et al. Dasatinib (BMS-354825) targets an earlier progenitor population than imatinib in primary CML but does not eliminate the quiescent fraction. *Blood.* 2006; 107(11):4532-4539.

45. DeAngelo DJ, Stone RM, Heaney ML, et al. Phase 1 clinical results with tandutinib (MLN518), a novel FLT3 antagonist, in patients with acute myelogenous leukemia or high-risk myelodysplastic syndrome: safety, pharmacokinetics, and pharmacodynamics. *Blood.* 2006;108(12):3674-3681.

46. Fiedler W, Mesters R, Tinnefeld H, et al. A phase 2 clinical study of SU5416 in patients with refractory acute myeloid leukemia. *Blood.* 2003;102(8): 2763-2767.

47. Loriaux MM, Levine RL, Tyner JW, et al. High-throughput sequence analysis of the tyrosine kinome in acute myeloid leukemia. *Blood.* 2008; 111(9):4788-4796.

Int J Hematol (2009) 90:471–475
DOI 10.1007/s12185-009-0427-x

CASE REPORT

Hairy cell leukemia responsive to anti-thymocyte globulin used as immunosuppressive therapy for aplastic anemia

Shiho Fujiwara · Hirosada Miyake · Kisato Nosaka · Minoru Yoshida · Sonoko Ishihara · Kentaro Horikawa · Yuji Yonemura · Kenichi Iyama · Hiroaki Mitsuya · Norio Asou

Received: 13 March 2009 / Revised: 14 July 2009 / Accepted: 6 September 2009 / Published online: 14 October 2009

Abstract Hairy cell leukemia (HCL) is occasionally misdiagnosed as aplastic anemia when only a few leukemic cells are present in the circulation. Here, we describe a patient with HCL who initially presented with pancytopenia and received a diagnosis of aplastic anemia. The patient was treated with immunosuppressive therapy including cyclosporine A and anti-thymocyte globulin (ATG). No blood cell transfusion was required for approximately 3 years after ATG therapy. She was referred to our hospital because of an abdominal mass and requiring periodic blood transfusions. A bone marrow biopsy at this time revealed proliferation of lymphocytes with a fried egg appearance and an increase in reticulin fibers that are typical findings of HCL. It is notable that our patient with a presumably long history of HCL and an increase in marrow reticulin fibers showed good recovery of hematopoiesis after cladribine therapy. Some HCL patients may receive an initial diagnosis of aplastic anemia and may show a good response to ATG masking the underlying HCL.

S. Fujiwara · H. Miyake · K. Nosaka · K. Horikawa · Y. Yonemura · H. Mitsuya · N. Asou (✉)
Department of Hematology,
Kumamoto University School of Medicine,
1-1-1 Honjo, Kumamoto 860-8556, Japan
e-mail: ktcnasou@gpo.kumamoto-u.ac.jp

M. Yoshida
Department of Medical Oncology,
Kumamoto Red Cross Hospital,
Kumamoto, Japan

S. Ishihara · K. Iyama
Department of Pathology,
Kumamoto University Hospital,
Kumamoto, Japan

Keywords Hairy cell leukemia · Aplastic anemia · Anti-thymocyte globulin · Pancytopenia · Splenomegaly

1 Introduction

Hairy cell leukemia (HCL) is a chronic B cell lymphoproliferative disorder. Although HCL accounts for 2–3% of all leukemia cases in western countries, the disease is rare in persons of Asian and African descent [1, 2]. Hairy cells are small lymphocytes with oval nuclei and abundant cytoplasm that possess characteristic hair-like surface projections. The typical presentation of HCL includes incidental findings of pancytopenia, splenomegaly, and inaspirable bone marrow [1–3]. Therefore, it is important to distinguish it from aplastic anemia or myelofibrosis. In this study, we present an HCL patient with pancytopenia who initially received a diagnosis of aplastic anemia, for which she was treated with immunosuppressive therapy including cyclosporine A (CyA) and anti-thymocyte globulin (ATG).

2 Case presentation

In December 2002, a 67-year-old Japanese woman was found to have mild pancytopenia during an annual health check. Her hemoglobin was 11.6 g/dL, platelet count 127×10^9/L, and leukocyte count 2.1×10^9/L, respectively.

In September 2003, she underwent a medical examination because of general fatigue. Her hemoglobin was 10.7 g/dL, platelet count 90×10^9/L, and leukocyte count 2.3×10^9/L with 27% neutrophils, 72% lymphocytes, and 1% monocytes. Immunophenotyping of peripheral blood

and marrow cells was not carried out at that time. Abdominal echography revealed moderate splenomegaly. Her bone marrow was hypoplastic and a diagnosis of aplastic anemia was made. No bone marrow biopsy was done at the time of this initial diagnosis. There was no history of exposure to chemicals, irradiation, or toxins, and she was not receiving any medications. Despite the treatment with CyA, danazol, and granulocyte colony-stimulating factor, her hemoglobin continued to gradually decrease and she received occasional red blood cell transfusions (Fig. 1). In January 2004, the patient needed both red blood cell and platelet transfusions (platelet count 19 × 10^9/L), and was treated with ATG (lymphoglobulin 10 mg/kg for 5 days). She needed no further blood transfusions for the next 32 months until December 2006 when she again started to receive red blood cell transfusions (Fig. 1). When periodic transfusions of red blood cells and platelets were resumed in October 2007, the patient had a feeling of abdominal fullness. In June 2008, she developed a compression fracture of the spine, and an abdominal computed tomography (CT) scan showed splenomegaly and lymph node swelling in the pancreas head (Fig. 2a). She was referred to our hospital in July 2008.

At the time of admission to our hospital, the patient had anemia, mild jaundice, splenomegaly (6 cm), an upper abdominal mass (3 cm), and purpura on both upper legs. Her hemoglobin was 8.4 g/dL, platelet count 27 × 10^9/L, leukocyte count 0.9 × 10^9/L with 49% neutrophils, 48% lymphocytes, 1% eosinophils, and 1% monocytes. A few small lymphocytes with cytoplasmic projections were seen in the peripheral blood (Fig. 3a). Blood chemistry showed abnormal findings: total protein 6.0 g/dL, albumin 3.8 g/dL, blood urea nitrogen 32.6 mg/dL, serum creatinine 1.23 mg/dL, total bilirubin 1.9 mg/dL, direct bilirubin 0.8 mg/dL, aspartate aminotransferase 41 U/L, alanine aminotransferase 35 U/L, lactate dehydrogenase 221 U/L (normal range 112–213 U/L), and soluble interleukin 2 receptor (sIL2R) 55,583 U/mL (normal range 333–587 U/mL). Bone marrow aspiration resulted in a dry tap. A bone marrow biopsy from the iliac crest revealed moderately hypercellularity and replacement of normal hematopoietic cells with abnormal small lymphocytes with abundant cytoplasm and oval nuclei, the so-called fried egg

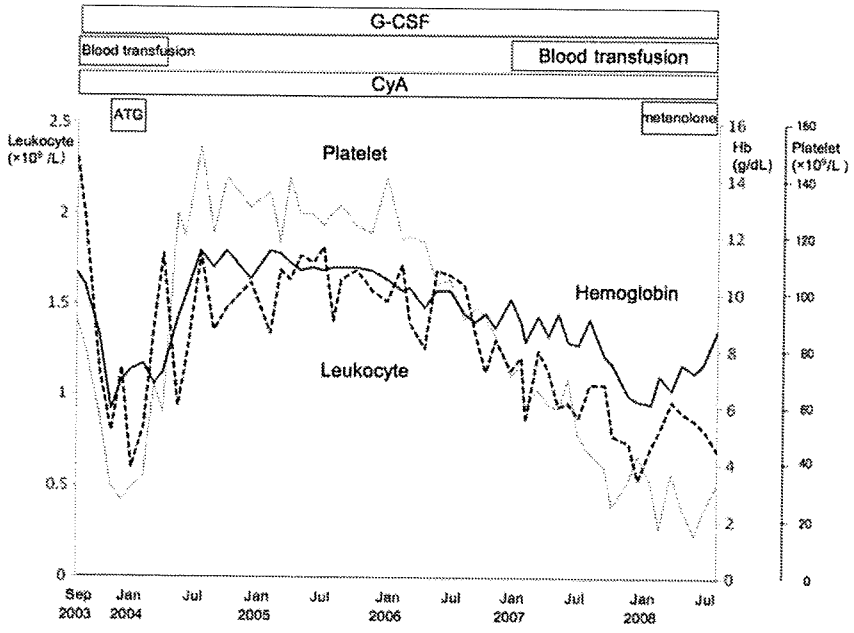

Fig. 1 Clinical course during immunosuppressive therapy for aplastic anemia. *Solid line* shows hemoglobin level, *dotted line* indicates platelet count, and *broken line* represents leukocyte count. *ATG* anti-thymocyte globulin, *CyA* cyclosporine A, *G-CSF* granulocyte colony-stimulating factor

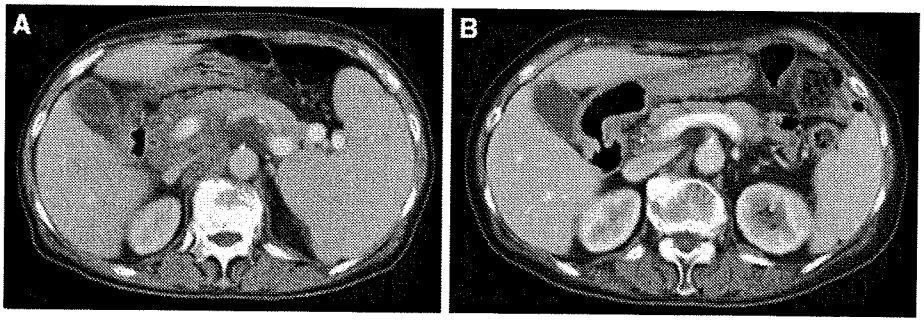

Fig. 2 Abdominal computed tomography (CT) scan. In July 2008, abdominal CT scan revealed lymph node swelling in the pancreas head and giant splenomegaly (**a**). The abdominal mass disappeared and the spleen reduced in size in January 2009 after cladribine therapy (**b**)

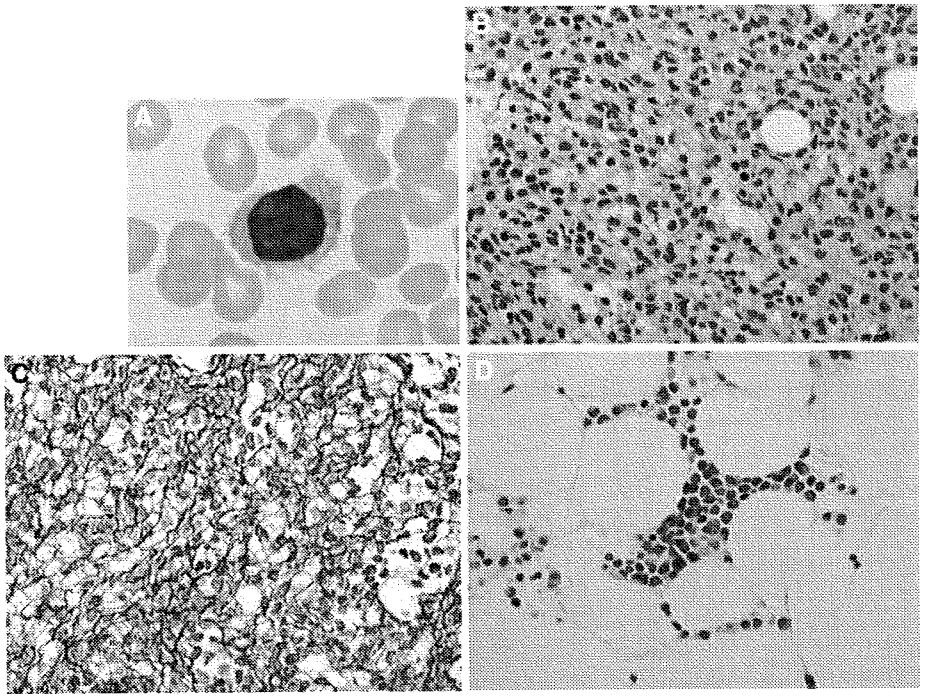

Fig. 3 Hairy cells in the peripheral blood and bone marrow. A hairy cell in the peripheral blood, with an eccentric round nucleus containing fine chromatin condensation and abundant cytoplasm with irregular fine surface projections (**a**). The lymphocytes in the bone marrow biopsy showed a fried egg appearance after routine hematoxylin and eosin staining (**b**) and increased reticulin fibers were detected after silver staining (**c**). A cluster of abnormal lymphocytes was retrospectively observed in the bone marrow clot on 2003 before ATG therapy (**d**). These lymphocytes were positive for CD20

appearance (Fig. 3b). Her marrow also contained increased reticulin fibers (Fig. 3c). The marrow reticulin content was graded as +1 according to Manoharan's scoring system [4]. A positive tartrate-resistant acid phosphatase stain of the bone marrow cells was not observed. The gated bone marrow lymphocytes (37%) were positive for CD19 (94%), CD20 (93%), immunoglobulin κ chain (67%), CD25 (83%), CD11c (99%), and CD103 (77%), but negative for λ chain (6%), CD23 (3%), and CD10 (1%). Flow cytometry analysis revealed that 2.7% of the peripheral blood cells were consistent with hairy cells based on the positive expression of CD19, CD25, CD11c, and CD103. Aspiration biopsy of the abdominal mass also revealed the proliferation of small lymphocytes with a fried egg appearance (data not shown). The patient was given a diagnosis of HCL. We retrospectively examined the bone marrow smears and histology of the bone marrow clots before ATG therapy in the previous hospital. A few lymphocytes with abundant cytoplasm and cytoplasmic projections were found in the bone marrow smears on 2003. In addition, the bone marrow clot in 2003 was hypocellular, but showed a cluster of abnormal lymphocytes, which were positive for CD20 (Fig. 3d).

After the discontinuation of CyA, the patient was treated with cladribine 0.12 mg/kg daily 2-h infusion for 5 days in August 2008 (Fig. 4). After one course of cladribine therapy, the abdominal mass and spleen were dramatically reduced in size and the patient no longer required blood transfusions (hemoglobin 9.2 g/dL, platelet count 99 $\times$ 10^9/L, leukocyte count 1.3 $\times$ 10^9/L). She received a second and third course of cladribine in September and November, respectively (Fig. 4). In January 2009, the abdominal mass had disappeared and the spleen was reduced in size on CT scan (Fig. 2b). Her hemoglobin was 13.2 g/dL, platelet count 97 $\times$ 10^9/L, and leukocyte count 1.8 $\times$ 10^9/L. Her sIL2R has decreased to 6,596 and 259 U/mL after the first and third courses of cladribine therapy, respectively (Fig. 4).

3 Discussion

In this study, we present an HCL patient who was treated with immunosuppressive therapy including CyA and ATG for 5 years due to a diagnosis of aplastic anemia. HCL is occasionally misdiagnosed as aplastic anemia, when there are only a few abnormal circulating cells [1, 2, 5, 6]. Hairy cells typically infiltrate the bone marrow and spleen, and to a lesser extent the lymph nodes, hence, many HCL patients present with splenomegaly and pancytopenia [1–3]. However, some patients with HCL manifest pancytopenia and bone marrow hyperplasia without an apparent increase in atypical cells [7]. In this patient, abdominal echography revealed splenomegaly in 2003. We, retrospectively, found abnormal lymphocytes with characteristic cytoplasmic projections in the bone marrow smears and a cluster of CD20-positive abnormal lymphocytes in the bone marrow clot in 2003. In addition, cladribine therapy resulted in significant recovery of hematopoietic cells in the peripheral blood. Therefore, it is likely that the patient had been suffering from HCL, since her initial presentation with pancytopenia although we cannot completely established the diagnosis of HCL at the time of ATG therapy.

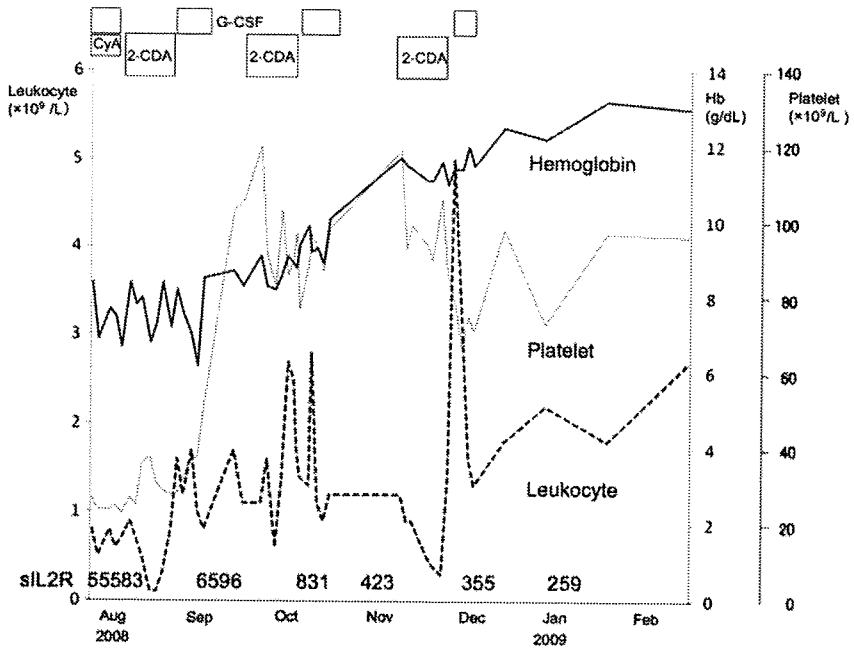

Fig. 4 Cladribine therapy for hairy cell leukemia. Cladribine (2-CDA) induced an increase in hemoglobin, platelet and leukocyte counts, and a decrease in serum levels of soluble interleukin-2 receptor (sIL2R), leading to the release from red blood cell and platelet transfusions. *Solid line* shows hemoglobin level, *dotted line* indicates platelet count, and *broken line* represents leukocyte count. *G-CSF* granulocyte colony-stimulating factor, *CyA* cyclosporine A

Table 1 Hairy cell leukemia patients treated with anti-thymocyte globulin

Case (references)	Age/sex	Hb (g/dL)	Plt ($\times 10^9$/L)	WBC	Splenomegaly	sIL2R (U/mL)	CD25	Response	
								ATG	Cladribine
1 (7)	54/M	5.3	18	0.5	+	23,087.8	+	+	+
2 (7)	58/F	4.7	13	0.3	+ (10 cm)	4,940[a]	+	+	ND
3 (2)	65/M	12.7	NA	2.0	−	NT	+	−	−
4[b]	68/F	8.4	27	0.9	+ (6 cm)	55,583	+	+	+

Hb hemoglobin, *Plt* platelet, *WBC* white blood cells, *sIL2R* soluble interleukin 2 receptor, *ATG* anti-thymocyte globulin, *NA* not available, *NT* not tested, *ND* not done

[a] sIL2R level was measured after ATG therapy in this patient

[b] Present case

It is well known that bone marrow biopsy is essential for diagnosing aplastic anemia to exclude myelofibrosis and neoplasms such as metastatic cancers. Bone marrow biopsy also reveals the characteristic histology of HCL: proliferation of abnormal lymphocytes with abundant cytoplasm (fried egg appearance) and increased reticulin fibers [1, 2]. In a study of simultaneous bone marrow aspirations and biopsies, 87 of 2,235 individuals resulted in dry taps (3.9%) [8]. Of these 87 dry taps, nine (10.3%) were diagnosed to have an HCL. Unfortunately, no bone marrow biopsy was performed in our patient until admission to our hospital. The presenting patient, therefore, confirms the importance of examining bone marrow biopsies in patients with pancytopenia.

After ATG therapy, the patient required no blood cell transfusion for approximately 3 years. Two other Japanese HCL patients also showed good responses to ATG given as immunosuppressive therapy for aplastic anemia, but an American patient with HCL failed to respond to ATG (Table 1) [2, 7]. The mechanism responsible for the effectiveness of ATG for pancytopenia in HCL patients remains to be determined. It is likely that ATG induces hematopoietic recovery by eliminating the HCL cells. ATG may exclude B cells as well as T cells [7, 9]. It is also possible that ATG may remove CD25-positive cells [9, 10]. HCL cells in all four patients treated with ATG were positive for CD25 (Table 1). It is notable that our patient who was presumed to have a long history of HCL and an increase in marrow reticulin fibers responded to cladribine and showed good recovery of hematopoiesis. sIL2R appears to be a good disease marker in CD25-positive HCL [11, 12]. In two of the HCL patients treated with ATG, sIL2R levels were extremely high (Table 1) and fell to normal levels after cladribine therapy [7].

Some HCL patients may initially receive a diagnosis of aplastic anemia and may show a good response to ATG, resulting in masking of the underlying HCL. Several bone marrow biopsies and measurement of sIL2R are important procedures for the accurate diagnosis of HCL.

Acknowledgments We thank Dr. Koichi Ohshima from Kurume University for his helpful discussion of this study. This work was supported in part by Grants-in-Aid for Scientific Research from the Japanese Ministry of Education, Culture, Sport, Science, and Technology, and Grants-in-Aid for Cancer Research from the Japanese Ministry of Health, Labor, and Welfare.

References

1. Allsup DJ, Cawley JC. The diagnosis and treatment of hairy-cell leukaemia. Blood Rev. 2002;16:255–62.
2. Wanko SO, de Castro C. Hairy cell leukemia: an elusive but treatable disease. Oncologist. 2006;11:780–9.
3. Tiacci E, Liso A, Piris M, Falini B. Evolving concepts in the pathogenesis of hairy-cell leukaemia. Nat Rev Cancer. 2006;6:437–48.
4. Manoharan A, Horsley R, Pitney WR. The reticulin content of bone marrow in acute leukaemia in adults. Br J Haematol. 1979;43:185–90.
5. Krause JR. Aplastic anemia terminating in hairy cell leukemia: a report of two cases. Cancer. 1984;53:1533–7.
6. Dixey JJ, Gazzard BG. Hairy cell leukaemia presenting as aplastic anaemia. J R Soc Med. 1983;76:427–8.
7. Sugimori C, Kaito K, Nakao S. Persistent remission after immunosuppressive therapy of hairy cell leukemia mimicking aplastic anemia: two case reports. Int J Hematol. 2003;77:391–4.
8. Humphries JE. Dry tap bone marrow aspiration: clinical significance. Am J Hematol. 1990;35:247–50.
9. Tsuge I, Kojima S. Comparison of antibody specificities of four anti-thymocyte/anti-lymphocyte globulin products. Curr Ther Res. 1995;56:671–7.
10. Bonnefoy-Berard N, Verrier B, Vincent C, Revillard JP. Inhibition of CD25 (IL-2R alpha) expression and T-cell proliferation by polyclonal anti-thymocyte globulins. Immunology. 1992;77:61–7.
11. Chilosi M, Semenzato G, Cetto G, Ambrosetti A, Fiore-Donati L, Perona G, et al. Soluble interleukin-2 receptors in the sera of patients with hairy cell leukemia: relationship with the effect of recombinant alpha-interferon therapy on clinical parameters and natural killer in vitro activity. Blood. 1987;70:1530–5.
12. Steis RG, Marcon L, Clark J, Urba W, Longo DL, Nelson DL, et al. Serum soluble IL-2 receptor as a tumor marker in patients with hairy cell leukemia. Blood. 1988;71:1304–9.

GENES, CHROMOSOMES & CANCER 49:237–241 (2010)

A Family Harboring a Germ-Line N-Terminal C/EBPα Mutation and Development of Acute Myeloid Leukemia with an Additional Somatic C-Terminal C/EBPα Mutation

Tomoko Nanri,[1] Naokuni Uike,[2] Toshiro Kawakita,[1] Eisaku Iwanaga,[1] Hiroaki Mitsuya,[1] and Norio Asou[1]*

[1]Department of Hematology, Kumamoto University School of Medicine, Kumamoto, Japan
[2]Department of Hematology, National Kyushu Cancer Center, Fukuoka, Japan

C/EBPα plays an essential role as a transcription factor in myeloid cell differentiation. Here, we describe a Japanese family in which two individuals with acute myeloid leukemia (AML) and one healthy individual had an identical 4-base pair insertion in the N-terminal region of *CEBPA* (350_351insCTAC), resulting in the termination at codon 107 (I68fsX107). The father and a son at diagnosis of AML had different in-frame insertion mutations in the C-terminal region of C/EBPα These C-terminal mutations disappeared upon remission in both patients. Interestingly, the father showed different in-frame insertion mutations in the C-terminal *CEBPA* at the time of diagnosis and relapse. These data strongly suggest that the N-terminal C/EBPα mutation predisposes to the occurrence of a C-terminal C/EBPα mutation as a secondary genetic hit, causing AML.

INTRODUCTION

Chromosomal translocations and point mutations of transcription factors involved in myeloid cell differentiation contribute to the molecular pathogenesis of acute myeloid leukemia (AML) (Asou, 2003; Tenen, 2003). Point mutations in transcription factors observed in patients with sporadic AML have also been identified in familial AMLs (Osato et al., 1999; Pabst et al., 2001; Michaud et al., 2002; Smith et al., 2004). Recently, five pedigrees of patients with AML carrying a germ-line mutation in *CEBPA*, a single-exon gene encoding transcription factor CCAAT enhancer-binding protein alpha (C/EBPα), have been reported (Smith et al., 2004; Sellick et al., 2005; Pabst et al., 2008; Renneville et al., 2009). C/EBPα consists of N-terminal transactivation domains and C-terminal basic and leucine-zipper regions necessary for specific DNA binding and dimerization, respectively (Nerlov, 2004). As C/EBPα-null mice lack mature neutrophils and eosinophils, C/EBPα is thought to play a central role in the regulation of myeloid differentiation (Zhang et al., 1997). Familial AML will provide a good opportunity to investigate the molecular mechanisms behind leukemogenesis in AML. Here, we describe a family in which two individuals developing AML had an identical germ-line N-terminal *CEBPA* mutation and a different acquired C-terminal *CEBPA* mutation.

MATERIALS AND METHODS

Patients and Cell Preparation

This study was approved by the Institutional Review Boards for the Protection of Human Subjects and Analysis of the Human Genome. Written informed consent was obtained from each individual according to the tenets of the revised Declaration of Helsinki. Mononuclear cells were isolated from peripheral blood or bone marrow samples. The patients were treated with intensive chemotherapy consisting of anthracyclines and cytarabine.

Supported by: Japanese Ministry of Education, Culture, Sport, Science and Technology; Cancer Research from Japanese Ministry of Health; Labor and Welfare; Japan Leukaemia Research Fund.

*Correspondence to: Norio Asou, Department of Hematology, Kumamoto University School of Medicine, 1-1-1 Honjo, Kumamoto 860-8556, Japan. E-mail: ktcnasou@gpo.kumamoto-u.ac.jp

Received 5 August 2009; Accepted 16 October 2009

DOI 10.1002/gcc.20734

Published online 1 December 2009 in Wiley InterScience (www.interscience.wiley.com).

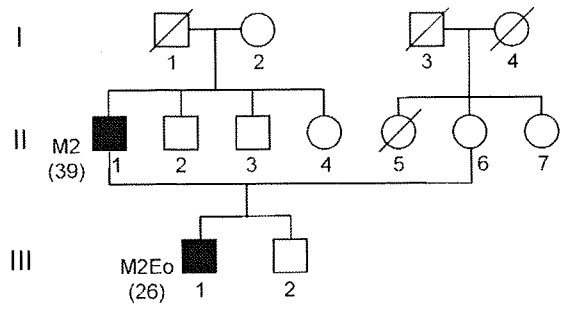

Figure 1. A pedigree harboring a germ-line N-terminal C/EBPα mutation. The propositus (Individual III-1) had AML M2Eo at the age of 26 years. His father (Individual II-1) had AML M2 at the age of 39 years. His younger brother (Individual III-2) aged 21 years has not developed AML.

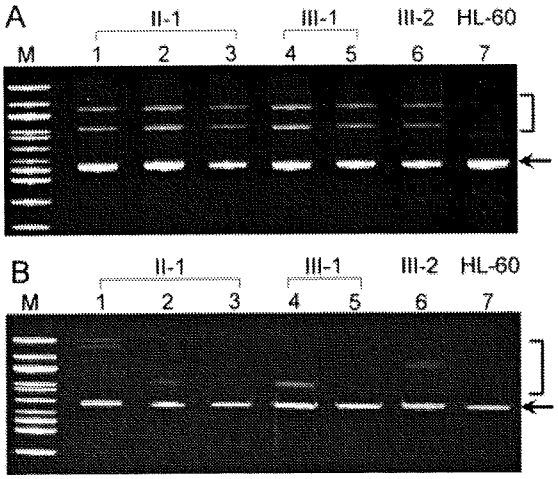

Figure 2. Polyacrylamide gel electrophoresis of *CEBPA* gene PCR products. PCR products from the N-terminal (A) and C-terminal (B) parts of the *CEBPA* gene were analyzed by polyacrylamide gel electrophoresis (PAGE). The mutated alleles are confirmed by the presence of heteroduplex bands (bracket) in addition to homoduplex bands of normal and/or inserted alleles (arrow). Lane M shows a 100-bp DNA ladder. Lane 1: bone marrow (BM) at diagnosis in the father (II-1); Lane 2: BM at relapse in the father; Lane 3: peripheral blood (PB) at second CR in the father; Lane 4: BM at diagnosis in the propositus (III-1); Lane 5: PB at CR in the proband; Lane 6: PB from the younger brother (III-2); Lane 7: HL-60 cell line served as a wild-type control. In the C-terminal part of *CEBPA*, the younger brother (III-2) showed a 6-bp insertion (730–731insCCCGCA) in the second transactivation domain. This insertion occurred on the allele without the N-terminal *CEBPA* mutation and corresponds to a previously reported polymorphism (Lin et al., 2005) (B).

Polymerase Chain Reaction

The *CEBPA* was amplified by genomic DNA polymerase chain reaction (PCR) in a DNA thermal cycler (Whatman Biometra, Goettingen, Germany) (Asou et al., 2007). Two overlapping primer pairs were the same as those designed by Pabst et al. (2001) and used to amplified the entire coding region of human *CEBPA*: PP1F 5′-TCGCCATGCCGGGAGAACTCTAAC-3′ (nucleotides 120–143) and PP1R 5′-CTGGTAAGGGAAGAGGCCGGCCAG-3′ (nucleotides 692–669), PP2F 5′-CCGCTGGTGATCAAGCAGGA-3′ (nucleotides 615–634) and PP2R 5′-CACGGTCTGGGCAAGCCTCGAGAT-3′ (nucleotides 1317–1294). An aliquot of each PCR product was size-fractionated in an 8% polyacrylamide gel electrophoresis (PAGE) (Nanri et al., 2005a). Mutations in the juxtamembrane and second tyrosine kinase domains of *FLT3*, exon 8, juxtamembrane, and second tyrosine kinase domains of the *KIT*, *MLL*, and *NPM1* genes were examined as previously described (Matsuno et al., 2003; Nanri et al., 2005b; Iwanaga et al., 2009).

DNA Sequencing

Amplified PCR products were bidirectionally sequenced by cycle sequencing (Applied Biosystems, Foster City, CA). To determine whether N- and C-terminal mutations occur in different alleles or a single allele, the whole *CEBPA* gene was amplified by PCR using primers PP1F and PP2R. PCR products were subcloned into pGEM-T Easy vector (Promega, Madison, WI) and subjected to cycle sequencing.

RESULTS

A 26-year-old Japanese man, Individual III-1, was diagnosed with M2Eo in 2004 (Fig. 1). His marrow showed 73.2% blasts including Auer rods and 6.8% eosinophils. Karyotypic and immunophenotypic analyses were not performed because of New Year holiday. Cryopreserved bone marrow cells showed none of the fusion transcripts, *AML1-MTG8*, *PML-RARA*, *PEBP2B-MYH11*, *MLL-AF4*, *MLL-AF9*, or *BCR-ABL*. He received autologous hematopoietic stem cell transplantation (HSCT) in the first complete remission (CR) and has been in continuous CR for more than 54 months. Sixteen years previously in 1988, his father, Individual II-1, was diagnosed with AML M2, at the age of 39 years (Fig. 1). His marrow was hypercellular, with 85.2% blasts containing Auer rods and aberrantly expressed CD7 antigen. Bone marrow cells showed a normal karyotype. Following a relapse 7 years after his first CR, he received autologous HSCT, after which he has been in a lasting CR.

Bone marrow cells at diagnosis in both patients (II-1 and III-1) showed abnormal PAGE profiles when compared with a wild-type control (Fig. 2A) and a 4-base pair insertion in the N-terminal region of the *CEBPA* (350_351insCTAC) (Fig. 3A). The corresponding protein is predicted to terminate prematurely at codon 107 (I68fsX107).

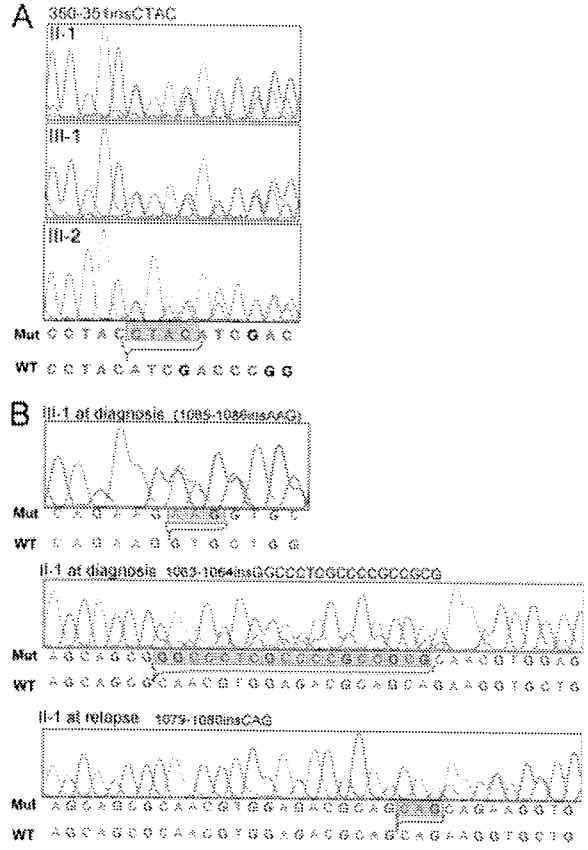

Figure 3. Sequencing analysis of the N- and C-terminal *CEBPA* in a pedigree. Bone marrow cells at diagnosis from the father (II-1) and the propositus (III-1), and peripheral blood cells from the younger brother (III-2) showed a 4-base pair insertion in the N-terminal region of *CEBPA* gene (350_351insCTAC). (B) Different in-frame insertion mutations in the C-terminal region of *CEBPA* gene were identified in both patients (II-1 and III-1) at diagnosis. The propositus (III-1) showed a 3-bp insertion, which comprised nucleotides 1085–1087 and resulted in an internal duplication of 3-bp. The father (II-1) had an 18-bp insertion. In addition, the father (II-1) showed different C-terminal *CEBPA* mutations at diagnosis and "relapse". The father showed a 3-bp insertion at nucleotide 1079 at relapse.

Peripheral blood cells obtained during CR in both patients also had the same mutation (Fig. 2A). In addition, peripheral blood cells from a younger brother, Individual III-2, unaffected by AML at 21 years of age also showed the same mutation (Figs. 2A and 3A). Both patients showed different in-frame insertion mutations in the C-terminal region of C/EBPα at diagnosis (Figs. 2B and 3B). These C-terminal *CEBPA* mutations were not found in peripheral blood cells during CR in either patient, indicating that these mutations in the C-terminal C/EBPα should be somatic mutations (Fig. 2B). In addition, the father showed different in-frame insertion mutations in the C-terminal *CEBPA* at the time of diagnosis and relapse (Figs. 2B and 3B). The N- and C-terminal mutations in both patients were observed on separate alleles because each subclone consisting of the whole *CEBPA* gene showed one of each mutation. No other mutations were identified in *FLT3*, *KIT*, *MLL*, or *NPM1* at diagnosis or relapse of the two patients (data not shown).

DISCUSSION

We present a family with AML harboring an identical germ-line N-terminal *CEBPA* mutation and different acquired C-terminal *CEBPA* mutations. This N-terminal mutation causes truncation of the 42-kDa C/EBPα protein and overproduction of a 30-kDa isoform, which lacks a transactivation domain and functions in a dominant negative fashion, causing a decrease in C/EBPα activity (Nerlov, 2004). The germ-line mutation found in the affected individuals is almost identical to those in the familial AMLs carrying a *CEBPA* mutation (Table 1) (Smith et al., 2004; Sellick et al., 2005; Pabst et al., 2008; Renneville et al., 2009). The *CEBPA* mutations in patients with sporadic AML are associated with FAB M1/M2 subtypes, presence of Auer rods, CD7 expression, normal karyotype, and a favorable prognosis (Gombart et al., 2002; Preudhomme et al., 2002; Snaddon et al., 2003; Frohling et al., 2004; Lin et al., 2005). The present familial AML with an N-terminal C/EBPα mutation further confirms this clinico-genetic correlation.

It is of note that different in-frame insertion mutations in the C-terminal region of C/EBPα were identified in both patients at diagnosis. These C-terminal mutations are predicted to prevent dimerization of C/EBPα because they disrupt the leucine zipper and therefore results in loss of function of the allele (Nerlov, 2004). These results indicate that the N-terminal C/EBPα mutation may predispose to the occurrence of a C-terminal C/EBPα mutation. High frequencies of biallelic N- and C-terminal mutations were observed in sporadic AML (Barjesteh van Waalwijk van Doorn-Khosrovani et al., 2003; Frohling et al., 2005; Lin et al., 2005; Shih et al., 2006). Recently, Wouters et al. (2009) reported that double *CEBPA* mutations were associated with a unique gene expression profile and favorable overall survival (OS), whereas AML with a single heterozygous *CEBPA* mutation did not express a discriminating signature and could not

TABLE 1. Clinical Profiles of AML Patients with a Germ-Line *CEBPA* Mutation

Pedigree	Patient no.	Age/Sex	FAB	N-Terminal mutation	C-Terminal mutation	Induction result	SCT	Relapse	1st CR duration (months)	Overall survival (months)
1	II-3	10/M	M1	212delC	1050–1085dup36-bp	CR	No	2nd	15	348+
	III-1	30/M	M2Eo	212delC	Absence	CR	No	No	20+	20+
	III-5	18/F	M2Eo	212delC	Absence	CR	No	No	20+	20+
2	III-1	34/M	AML	217–218insC	ND	ND	No	ND	ND	13
	IV-2	25/M	M4Eo	217–218insC	1071–1077del GAGACGCins CTGGAGGCCA	CR	2 auto	2nd	6	216+
	IV-4	24/M	M1	217–218insC	1071–1072insGAC	CR	Auto	No	132+	132+
	V-1	4/M	M1	217–218insC	ND	CR	Auto	2nd	>72	168+
3	I-2	46/F	M2	291delC	ND	CR	No	Yes	7	9
	II-2	40/F	M1Eo	291delC	1086–1087insCAG	CR	Auto	No	15+	15+
4	I-2	42/M	M1	465–466insT	1207G>C:1210A>C	NR	No	ND	0	1
	II-1	27/F	M2Eo	465–466insT	1089–1090insAAG	CR	Auto	No	16+	16+
5	I-2	23/F	M1	217–218insC	1083–1085delAAG	CR	Auto	3rd	168	228+
	II-2	5/M	M1	217–218insC	1065–1066insGGG	CR	CBT	Yes	13	60+
6[a]	II-1	39/M	M2	350–351insCTAC	1063–1064ins18-bp/ 1079–1080insCAG	CR	Auto	Yes	84	253+
	III-1	26/M	M2Eo	350–351insCTAC	1085–1086insAAG	CR	Auto	No	54+	55+

FAB, French-American-British classification; CR, complete remission; NR, no response; ND, not determined; SCT, stem cell transplantation; auto, autologous SCT; CBT, cord blood transplantation; Pedigree 1, Smith et al., 2004; Pedigree 2, Sellick et al., 2005; Pedigrees 3 and 4, Pabst et al., 2008; Pedigree 5, Renneville et al., 2009.

[a]Present pedigree.

be distinguished from wild type of *CEBPA* cases with respect to OS.

Interestingly, the father showed different in-frame insertion mutations in the C-terminal *CEBPA* at the time of diagnosis and relapse. In contrast, none of the patients with sporadic AML developed a novel C/EBPα mutation at relapse, indicating that the *CEBPA* mutation is probably a primary change in the development of AML, but does not play a role in the progression of the disease (Lin et al., 2005, 2006; Shih et al., 2006). Both familial and sporadic AML patients with C/EBPα mutation have very good OS. However, 7 of 13 patients with familial AML relapsed and four had several relapses (Table 1) (Smith et al., 2004; Sellick et al., 2005; Pabst et al., 2008). These high frequencies of recurrences, despite a good OS, are generally unusual in sporadic AML. Moreover, three affected patients had unusually late relapse, after more than 6 years from first CR (Table 1) (Sellick et al., 2005; Pabst et al., 2008). Hematopoietic stem cells retain the germ-line N-terminal *CEBPA* mutation in affected individuals even in CR. During these intervals, familial members carrying an N-terminal *CEBPA* mutation may acquire a new C-terminal *CEBPA* mutation. At "relapse," although their leukemic cells showed similar morphology and immunophenotype as at the initial diagnosis, they might have developed a second new AML harboring a different C-terminal C/EBPα mutation.

Among patients with familial as well as sporadic AML, alterations of the *FLT3*, *MLL*, and *NRAS* genes are not commonly seen in combination with an inactivating *CEBPA* mutation (Barjesteh van Waalwijk van Doorn-Khosrovani et al., 2003; Frohling et al., 2004; Smith et al., 2004; Sellick et al., 2005; Lin et al., 2006; Pabst et al., 2008; Renneville et al., 2009). These observations suggest that N- and C-terminal biallelic mutations in the *CEBPA* are sufficient for the development of AML. High penetration rates and relatively young onset of AML in families with an N-terminal C/EBPα mutation were observed (Smith et al., 2004; Sellick et al., 2005; Pabst et al., 2008; Renneville et al., 2009). In contrast, approximately one-third of the affected members in families with an AML1/RUNX1 mutation developed AML after a long latency (Michaud et al., 2002; Asou, 2003). It is of note that point mutations in the *AML1* gene as well as *AML1*-associated chromosomal translocations require subsequent genetic alterations to cause AML (Matsuno et al., 2003; Nanri et al., 2005b). A recent study using a 30-kDa C/EBPα knock in mutation mimicking the most prevalent *CEBPA* biallelic mutations observed in patients with AML causes myeloid leukemia with full

penetrance in a mouse model (Kirstetter et al., 2008). This study indicates that the N-terminal C/EBPα mutation confers an increased risk for the occurrence of a C-terminal C/EBPα mutation as a second genetic hit, eventually leading to AML after a long latency.

ACKNOWLEDGMENTS

The authors are grateful to Dr. Motomi Osato, National University of Singapore, for his helpful discussions. They also thank Ms. Maki Ichinomiya-Nakayama for technical assistance.

REFERENCES

Asou N. 2003. The role of a Runt domain transcription factor AML1/RUNX1 in leukemogenesis and its clinical implications. Crit Rev Oncol Hematol 45:129–150.

Asou N, Yanagida M, Huang L, Yamamoto M, Shigesada K, Mitsuya H, Ito Y, Osato M. 2007. Concurrent transcriptional deregulation of AML1/RUNX1 and GATA factors by the AML1-TRPS1 chimeric gene in t(8;21)(q24;q22) acute myeloid leukemia. Blood 109:4023–4027.

Barjesteh van Waalwijk van Doorn-Khosrovani S, Erpelinck C, Meijer J, van Oosterhoud S, van Putten WL, Valk PJ, Berna Beverloo H, Tenen DG, Lowenberg B, Delwel R. 2003. Biallelic mutations in the CEBPA gene and low CEBPA expression levels as prognostic markers in intermediate-risk AML. Hematol J 4:31–40.

Frohling S, Schlenk RF, Stolze I, Bihlmayr J, Benner A, Kreitmeier S, Tobis K, Dohner H, Dohner K. 2004. CEBPA mutations in younger adults with acute myeloid leukemia and normal cytogenetics: Prognostic relevance and analysis of cooperating mutations. J Clin Oncol 22:624–633.

Frohling S, Schlenk RF, Krauter J, Thiede C, Ehninger G, Haase D, Harder L, Kreitmeier S, Scholl C, Caligiuri MA, Bloomfield CD, Döhner H, Döhner K. 2005. Acute myeloid leukemia with deletion 9q within a noncomplex karyotype is associated with CEBPA loss-of-function mutations. Genes Chromosomes Cancer 42:427–432.

Gombart AF, Hofmann WK, Kawano S, Takeuchi S, Krug U, Kwok SH, Larsen RJ, Asou H, Miller CW, Hoelzer D, Koeffler HP. 2002. Mutations in the gene encoding the transcription factor CCAAT/enhancer binding protein alpha in myelodysplastic syndromes and acute myeloid leukemias. Blood 99:1332–1340.

Iwanaga E, Nanri T, Matsuno N, Kawakita T, Mitsuya H, Asou N. 2009. A JAK2-V617F activating mutation in addition to KIT and FLT3 mutations is associated with clinical outcome in patients with t(8;21)(q22;q22) acute myeloid leukemia. Haematologica 94:433–435.

Kirstetter P, Schuster MB, Bereshchenko O, Moore S, Dvinge H, Kurz E, Theilgaard-Monch K, Mansson R, Pedersen TA, Pabst T, Schrock E, Porse BT, Jacobsen SE, Bertone P, Tenen DG, Nerlov C. 2008. Modeling of C/EBPα mutant acute myeloid leukemia reveals a common expression signature of committed myeloid leukemia-initiating cells. Cancer Cell 13:299–310.

Lin LI, Chen CY, Lin DT, Tsay W, Tang JL, Yeh YC, Shen HL, Su FH, Yao M, Huang SY, Tien HF. 2005. Characterization of CEBPA mutations in acute myeloid leukemia: Most patients with CEBPA mutations have biallelic mutations and show a distinct immunophenotype of the leukemic cells. Clin Cancer Res 11:1372–1379.

Lin LI, Lin TC, Chou WC, Tang JL, Lin DT, Tien HF. 2006. A novel fluorescence-based multiplex PCR assay for rapid simultaneous detection of CEBPA mutations and NPM mutations in patients with acute myeloid leukemias. Leukemia 20:1899–1903.

Matsuno N, Osato M, Yamashita N, Yanagida M, Nanri T, Fukushima T, Motoji T, Kusumoto S, Towatari M, Suzuki R, Naoe T, Nishii K, Shigesada K, Ohno R, Mitsuya H, Ito Y, Asou N. 2003. Dual mutations in the AML1 and FLT3 genes are associated with leukemogenesis in acute myeloblastic leukemia of the M0 subtype. Leukemia 17:2492–2499.

Michaud J, Wu F, Osato M, Cottles GM, Yanagida M, Asou N, Shigesada K, Ito Y, Benson KF, Raskind WH, Rossier C, Antonarakis SE, Israels S, McNicol A, Weiss H, Horwitz M, Scott HS. 2002. In vitro analyses of known and novel RUNX1/AML1 mutations in dominant familial platelet disorder with predisposition to acute myelogenous leukemia: Implications for mechanisms of pathogenesis. Blood 99:1364–1372.

Nanri T, Matsuno N, Kawakita T, Mitsuya H, Asou N. 2005a. Imatinib mesylate for refractory acute myeloblastic leukemia harboring inv(16) and a C-KIT exon 8 mutation. Leukemia 19:1673–1675.

Nanri T, Matsuno N, Kawakita T, Suzushima H, Kawano F, Mitsuya H, Asou N. 2005b. Mutations in the receptor tyrosine kinase pathway are associated with clinical outcome in patients with acute myeloblastic leukemia harboring t(8;21)(q22;q22). Leukemia 19:1361–1366.

Nerlov C. 2004. C/EBPα mutations in acute myeloid leukaemias. Nat Rev Cancer 4:394–400.

Osato M, Asou N, Abdalla E, Hoshino K, Yamasaki H, Okubo T, Suzushima H, Takatsuki K, Kanno T, Shigesada K, Ito Y. 1999. Biallelic and heterozygous point mutations in the runt domain of the AML1/PEBP2αB gene associated with myeloblastic leukemias. Blood 93:1817–1824.

Pabst T, Mueller BU, Zhang P, Radomska HS, Narravula S, Schnittger S, Behre G, Hiddemann W, Tenen DG. 2001. Dominant-negative mutations of CEBPA, encoding CCAAT/enhancer binding protein-alpha (C/EBPα), in acute myeloid leukemia. Nat Genet 27:263–270.

Pabst T, Eyholzer M, Haefliger S, Schardt J, Mueller BU. 2008. Somatic CEBPA mutations are a frequent second event in families with germline CEBPA mutations and familial acute myeloid leukemia. J Clin Oncol 26:5088–5093.

Preudhomme C, Sagot C, Boissel N, Cayuela JM, Tigaud I, de Botton S, Thomas X, Raffoux E, Lamandin C, Castaigne S, Fenaux P, Dombret H; ALFA Group. 2002. Favorable prognostic significance of CEBPA mutations in patients with de novo acute myeloid leukemia: A study from the Acute Leukemia French Association (ALFA). Blood 100:2717–2723.

Renneville A, Mialou V, Philippe N, Kagialis-Girard S, Biggio V, Zabot MT, Thomas X, Bertrand Y, Preudhomme C. 2009. Another pedigree with familial acute myeloid leukemia and germline CEBPA mutation. Leukemia 23:804–806.

Sellick GS, Spendlove HE, Catovsky D, Pritchard-Jones K, Houlston RS. 2005. Further evidence that germline CEBPA mutations cause dominant inheritance of acute myeloid leukaemia. Leukemia 19:1276–1278.

Shih LY, Liang DC, Huang CF, Wu JH, Lin TL, Wang PN, Dunn P, Kuo MC, Tang TC. 2006. AML patients with CEBPα mutations mostly retain identical mutant patterns but frequently change in allelic distribution at relapse: A comparative analysis on paired diagnosis and relapse samples. Leukemia 20:604–609.

Smith ML, Cavenagh JD, Lister TA, Fitzgibbon J. 2004. Mutation of CEBPA in familial acute myeloid leukemia. N Engl J Med 351:2403–2407.

Snaddon J, Smith ML, Neat M, Cambal-Parrales M, Dixon-McIver A, Arch R, Amess JA, Rohatiner AZ, Lister TA, Fitzgibbon J. 2003. Mutations of CEBPA in acute myeloid leukemia FAB types M1 and M2. Genes Chromosomes Cancer 37:72–78.

Tenen DG. 2003. Disruption of differentiation in human cancer: AML shows the way. Nat Rev Cancer 3:89–101.

Wouters BJ, Lowenberg B, Erpelinck-Verschueren CA, van Putten WL, Valk PJ, Delwel R. 2009. Double CEBPA mutations, but not single CEBPA mutations, define a subgroup of acute myeloid leukemia with a distinctive gene expression profile that is uniquely associated with a favorable outcome. Blood 113:3088–3091.

Zhang DE, Zhang P, Wang ND, Hetherington CJ, Darlington GJ, Tenen DG. 1997. Absence of granulocyte colony-stimulating factor signaling and neutrophil development in CCAAT enhancer binding protein alpha-deficient mice. Proc Natl Acad Sci USA 94:569–574.

Stem cell exhaustion due to Runx1 deficiency is prevented by Evi5 activation in leukemogenesis

Bindya Jacob,[1,2] Motomi Osato,[1,2] Namiko Yamashita,[1] Chelsia Qiuxia Wang,[1] Ichiro Taniuchi,[3] Dan R. Littman,[4] Norio Asou,[5] and Yoshiaki Ito[1,2]

[1]Institute of Molecular and Cell Biology, Singapore; [2]Cancer Science Institute of Singapore, National University of Singapore, Singapore; [3]RIKEN, Research Center for Allergy and Immunology, Yokohama, Kanagawa, Japan; [4]Howard Hughes Medical Institute, Skirball Institute of Biomolecular Medicine, New York University, NY; and [5]Department of Hematology, Kumamoto University School of Medicine, Kumamoto, Japan

The *RUNX1/AML1* gene is the most frequently mutated gene in human leukemia. Conditional deletion of *Runx1* in adult mice results in an increase of hematopoietic stem cells (HSCs), which serve as target cells for leukemia; however, *Runx1*$^{-/-}$ mice do not develop spontaneous leukemia. Here we show that maintenance of *Runx1*$^{-/-}$ HSCs is compromised, progressively resulting in HSC exhaustion. In leukemia development, the stem cell exhaustion was rescued by additional genetic changes. Retroviral insertional mutagenesis revealed *Evi5* activation as a cooperating genetic alteration and *EVI5* overexpression indeed prevented *Runx1*$^{-/-}$ HSC exhaustion in mice. Moreover, *EVI5* was frequently overexpressed in human RUNX1-related leukemias. These results provide insights into the mechanism for maintenance of preleukemic stem cells and may provide a novel direction for therapeutic applications. (Blood. 2010;115:1610-1620)

Introduction

The *RUNX1/AML1* gene encodes the DNA binding α subunit of heterodimeric Runt domain transcription factor, PEBP2/CBF.[1] RUNX1 and its partner protein, the non-DNA binding β subunit (PEBP2β/CBFβ), are essential for definitive hematopoiesis and are frequently targeted in human leukemia.[2-4] *RUNX1* and *CBFB* are involved in chromosomal translocations, generating fusion proteins that inhibit the activity of wild-type RUNX1 in a dominant-negative manner.[5,6] Biallelic point mutations of *RUNX1* are frequently found in the acute myeloid leukemia (AML) M0 subtype and familial platelet disorder with predisposition to AML. Monoallelic mutations are found in sporadic myelodysplastic syndrome and AML.[7-10] These point mutations make the RUNX1 protein nonfunctional. Hence, loss-of-function of RUNX1 is considered to be the common underlying mechanism for RUNX1-related leukemias.

Despite the prevalence of RUNX1 loss-of-function mutations or dominant-negative fusion proteins, the *RUNX1* alteration per se does not cause leukemia. Rather, cells with loss-of-function of RUNX1 remain leukemia-prone and only with acquisition of additional hits do they become fully leukemic.[11-14] Conditional deletion of *Runx1* in adult mice results in an expansion of immunophenotypically defined hematopoietic stem cell (HSC) compartment and an accumulation of megakaryoblasts and lymphoid progenitors.[15-17] The expansion of Runx1-deficient HSC/progenitor compartment is due to higher self-renewal and antiapoptotic properties and results in predisposition to leukemia.[18] However, surprisingly, despite the increased number of stem cells, Growney et al[16] reported that conditional *Runx1* knockout bone marrow (BM) cells are outcompeted by simultaneously transplanted wild-type BM cells in competitive repopulation assay, indicating that Runx1-deficient cells are compromised in reconstituting hematopoiesis in the recipient mice. Also, except for one group describing that *Runx1* conditional knockout mice developed lymphoma at later stages of life,[17] other groups reported that leukemia/lymphoma did not develop spontaneously. The above studies indicate increased leukemia susceptibility in Runx1-deficient conditions, and at the same time clearly suggest that Runx1-deficient cells require additional genetic changes for leukemic transformation.

Retroviral insertional mutagenesis (RIM) is a powerful tool to identify oncogenes and tumor suppressor genes.[19] Injection of replication-competent retrovirus into newborn mice leads to integration of virus into the host genome and activation of oncogenes or disruption of tumor suppressor genes, resulting in leukemia or lymphoma. Retrovirus usually hits multiple genes to induce leukemia or lymphoma.[20-23] RIM on conditional *Runx1* knockout mice provides an excellent system to identify genes that cooperate with loss-of-function of Runx1 to promote leukemogenesis. Previous RIM studies on heterozygous *Runx1* knockout mice have revealed the alterations of the *Ras* gene family and its upstream factors such as *c-Kit* and *Flt-3* as candidate "second hits" in leukemogenesis. These genes are in fact frequently mutated in human RUNX1-related leukemias.[18,22,24]

In this study, we show that Runx1 deficiency in HSCs leads to the phenomenon called "stem cell exhaustion" after the initial expansion. Runx1-deficient stem cell maintenance was compromised, probably due to defective niche interaction, resulting in decline of stem/progenitor cell numbers and decreasing contribution of these stem cells to blood cell production. We employed RIM on conditional *Runx1* knockout mice and identified overexpression of *Evi5* as an additional genetic alteration that prevents the stem cell exhaustion caused by Runx1 deficiency. Together, these 2 genetic alterations maintain an expanded pool of aberrant

Submitted July 12, 2009; accepted November 9, 2009. Prepublished online as *Blood* First Edition paper, December 14, 2009; DOI 10.1182/blood-2009-07-232249.

The online version of this article contains a data supplement.

The publication costs of this article were defrayed in part by page charge payment. Therefore, and solely to indicate this fact, this article is hereby marked "advertisement" in accordance with 18 USC section 1734.

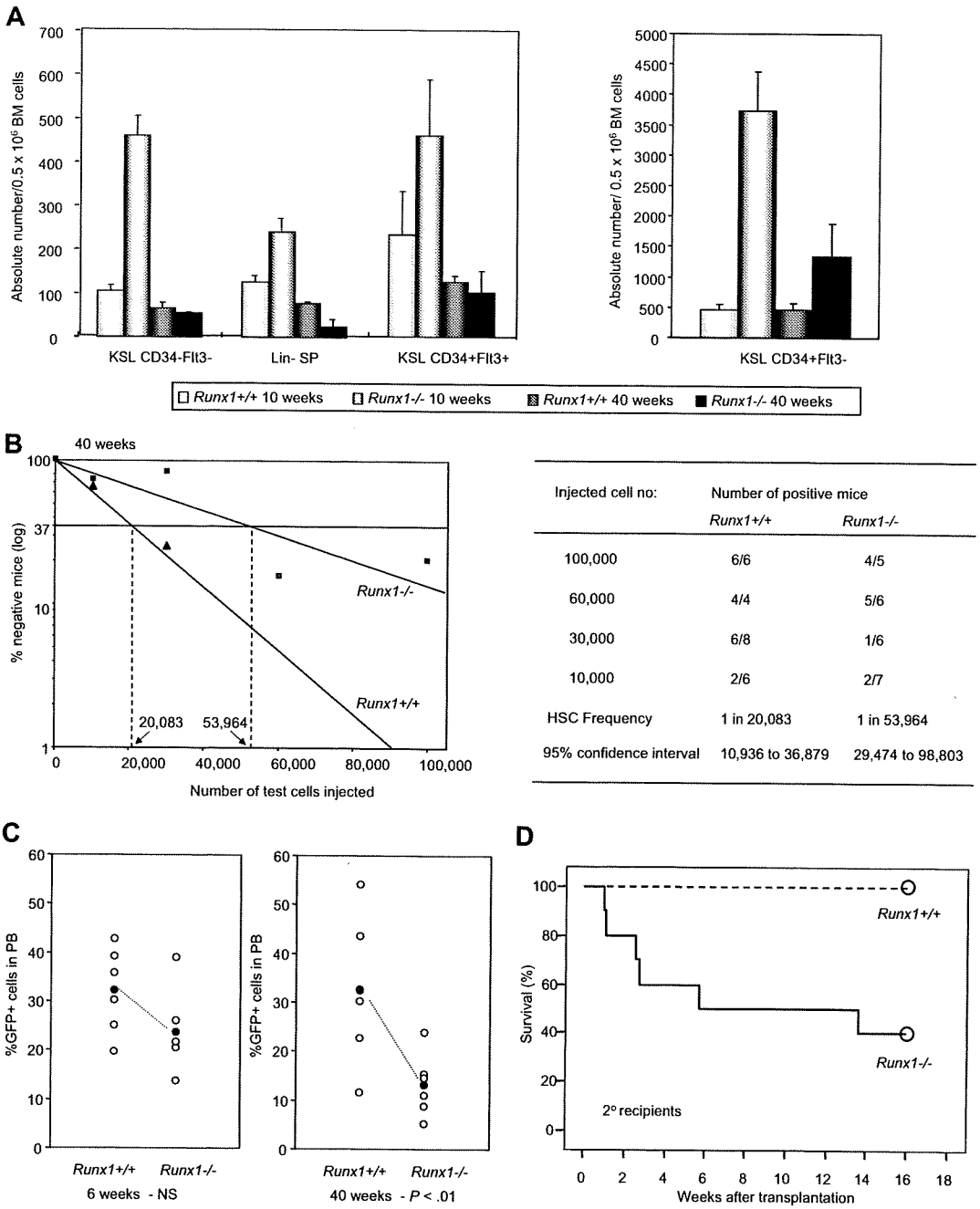

Injected cell no:	Number of positive mice	
	Runx1+/+	*Runx1-/-*
100,000	6/6	4/5
60,000	4/4	5/6
30,000	6/8	1/6
10,000	2/6	2/7
HSC Frequency	1 in 20,083	1 in 53,964
95% confidence interval	10,936 to 36,879	29,474 to 98,803

Figure 1. *Runx1*$^{-/-}$ status leads to stem cell exhaustion. (A) Absolute number of KSL CD34$^-$Flt3$^-$ cells, Lin$^-$ SP cells, KSL CD34$^+$Flt3$^+$ cells and KSL CD34$^+$Flt3$^-$ cells per 0.5 million BM cells from *Runx1*$^{+/+}$ and *Runx1*$^{-/-}$ mice of 2 distinct ages (10 and 40 weeks old). Each group comprises 3 to 4 mice. (B) Limiting dilution analysis using varying numbers of BM cells from 40-week-old CD45.2$^+$ *Runx1*$^{+/+}$ (▲), or *Runx1*$^{-/-}$ (■) mice. Mice were considered negative when the percent chimerism was less than 1%. Left panel: estimated frequencies of the repopulating cells are indicated as vertical dashed lines (1 repopulating cell per indicated numbers of BM cells) for each genotype. Right panel: for each indicated number of transplanted cells from CD45.2$^+$ *Runx1*$^{+/+}$ or *Runx1*$^{-/-}$ mice, the proportion of mice that are positive for test CD45.2$^+$ cells is given as (number of positive mice)/(number of analyzed mice). Frequencies of HSCs were calculated using Poisson statistics. (C) GFP chimerism in PB of recipients of *Runx1*$^{+/+}$ (n = 6) and *Runx1*$^{-/-}$ (n = 6) cells at 6 and 40 weeks after transplantation. Each open circle represents data from an individual mouse and each closed circle is the average of a cohort. Statistical difference using unpaired Student *t* test is given at the bottom. NS indicates not significant. (D) Kaplan-Meier survival curves of secondary recipients of mock MIG vector–transfected *Runx1*$^{+/+}$ (dashed line; n = 10) and *Runx1*$^{-/-}$ (solid line; n = 10) BM cells. Circles represent end point of analysis.

stem/progenitor cells, which may act as targets for further oncogenic hits.

Methods

Mice

The mice harboring *Runx1* allele with exon 4 flanked by loxP sites (*Runx1*$^{F/+}$) were generated,[25] backcrossed against C57BL/6 mice for 3 generations, and then intercrossed to obtain *Runx1*$^{F/F}$ mice. They were crossed with interferon-inducible *Mx-Cre* transgenic mice,[26] a gift from Dr K. Rajewsky, to generate *Runx1*$^{F/F}$–Tg(*Mx1-Cre*) mice. For further details, see supplemental Methods (available on the *Blood* website; click on the Supplemental Materials link at the top of the online article). All mice were maintained in the Biological Resource Center (BRC), Biopolis, Singapore, and all animal experiments followed the strict guidelines set by the National Advisory Committee for Laboratory Animal Research (NACLAR) and were approved by the BRC Institutional Animal Care and Use Committee.

Retroviral insertional mutagenesis

Runx1$^{F/F}$–Tg(*Mx1-Cre*) and *Runx1*$^{F/F}$ mice were mated, and progenies were injected with MoMuLV virus 3 days after birth and with polyinosinic-polycytidylic acid at 1 month of age. Retrovirus-injected *Runx1*$^{-/-}$ mice and *Runx1*$^{+/+}$ littermates were monitored by examining their health condition and by weekly checking of complete blood cell count using an automatic hematology analyzer (Celltac alpha MEK-6358; Nihon Kohden). Necropsy of diseased mice, hematology analysis, and identification of RIS using inverse polymerase chain reaction (PCR) were carried out as previously described.[22,23]

Flow cytometric analysis

Flow cytometric analysis was performed using a fluorescence-activated cell sorter (FACS) Vantage instrument as previously described.[18,22] Monoclonal antibodies were usually purchased from BD Biosciences (supplemental Methods).

Patient samples

Thirty-five human patients with leukemia belonging to the following categories were screened for expression level of *EVI5*: AML with t(8;21) (n = 9); inv(16) (n = 7); other AML (n = 10); chronic myeloid leukemia (CML) blast crisis (n = 6); and complete remission from AML (n = 3). Each patient gave informed consent to this study based on the tenets of the revised Helsinki protocol produced by the Institutional Committees for the Protection of Human Subjects and Analysis of the Human Genome. All studies of human samples were approved by the institutional review board of Kumamoto University Hospital.

Additional procedures

For complete information on bone marrow transplantation (BMT) procedures; plasmid construction, retroviral transduction, and in vitro cell culture assays; quantitative real-time PCR (qRT-PCR); luciferase assay; in vivo homing assay; and the BrdU incorporation assay, see the supplemental Methods.

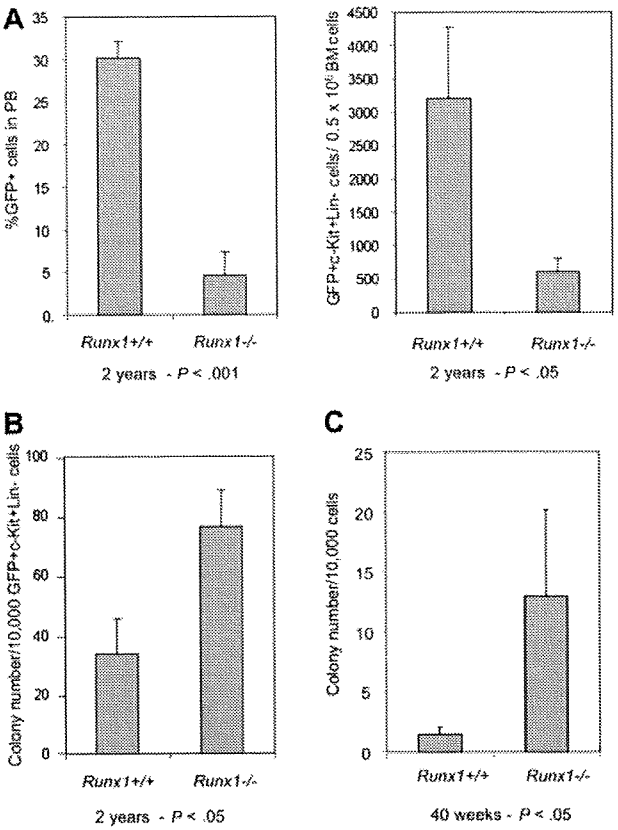

Figure 2. Aged *Runx1*$^{-/-}$ stem/progenitor cells maintain proliferative ability. (A) Graphs showing percentage of GFP$^+$ cells in PB and number of GFP$^+$c-Kit$^+$Lin$^-$ cells in BM of recipients of *Runx1*$^{+/+}$ (n = 3) and *Runx1*$^{-/-}$ (n = 3) BM cells, 2 years after transplantation. (B) Colony assay of GFP$^+$c-Kit$^+$Lin$^-$ cells from recipients of *Runx1*$^{+/+}$ (n = 3) and *Runx1*$^{-/-}$ (n = 3) BM cells, 2 years after transplantation. (C) Colony assay of KSL cells from 40-week-old mice, after 30 days of long-term culture on OP9 stromal cells. Statistical differences using the unpaired Student *t* test are given at the bottom.

Results

Runx1$^{-/-}$ stem/progenitor cell population declines after the initial expansion

Runx1 knockout (*Runx1*$^{-/-}$) BM cells, generated by Cre-recombinase–mediated knockout of *Runx1*, show an increase in hematopoietic stem/progenitor cell fraction compared with control wild-type (*Runx1*$^{+/+}$) mice. However, we found that *Runx1*$^{-/-}$ HSC expansion is followed by exhaustion, resulting in a progressive decline of stem/progenitor cell numbers. At 10 weeks of age, *Runx1*$^{-/-}$ mice showed a significant increase in long-term HSCs (c-Kit$^+$Sca1$^+$Lineage$^-$ [KSL] CD34$^-$Flt3$^-$), short-term HSCs (KSL CD34$^+$Flt3$^-$), and multipotential progenitors (KSL CD34$^+$Flt3$^+$). However, at 40 weeks of age, *Runx1*$^{-/-}$ stem/progenitor cell numbers declined significantly and were equivalent to or lesser than corresponding *Runx1*$^{+/+}$ cell numbers (Figure 1A, supplemental Figure 1). Side population analysis of lineage-negative cells (lineage-SP) also showed a similar trend of expansion of *Runx1*$^{-/-}$ HSCs at 10 weeks, followed by decline at 40 weeks (Figure 1A). To analyze the number of functional competitive repopulating units (CRUs) in aged (40 weeks old) *Runx1*$^{-/-}$ and *Runx1*$^{+/+}$ mice, we carried out limiting dilution BMT. The frequency of CRUs in BM of aged *Runx1*$^{-/-}$ mice was 1 in 53 964, lower than the frequency, 1 in 20 083, in *Runx1*$^{+/+}$ littermate controls (Figure 1B). These results suggest that stem cell exhaustion may occur in *Runx1*$^{-/-}$ mice.

The decline of *Runx1*$^{-/-}$ HSCs is further observed in another BMT experiment. In the recipient mice that underwent transplantation with BM cells from *Runx1*$^{-/-}$ and *Runx1*$^{+/+}$ mice transfected with MIG (MSCV-IRES-GFP) retroviral vector expressing enhanced green fluorescent protein (EGFP) as a surrogate marker, contribution of donor cells to hematopoiesis was monitored periodically by the percentage of GFP$^+$ cells in the peripheral blood (PB). At 6 weeks after transplantation, the GFP chimerism in PB of the recipients (n = 6) of *Runx1*$^{+/+}$ and *Runx1*$^{-/-}$ cells was comparable, with a mean value of 32.1% and 23.6% respectively. After 40 weeks, the mean GFP chimerism in the recipients of *Runx1*$^{+/+}$ remained the same at 32.5%, whereas it was significantly lower ($P < .01$) at 13.1% in the recipients of *Runx1*$^{-/-}$ cells (Figure 1C). By 2 years after transplantation, the GFP chimerism in PB of recipients of *Runx1*$^{-/-}$ cells dropped even further. There was also a concomitant decrease in absolute number of immature *Runx1*$^{-/-}$ (c-Kit$^+$Lineage$^-$GFP$^+$) cells in the BM of the recipients, again suggesting stem cell exhaustion (Figure 2A).

To ascertain the phenomenon of *Runx1*$^{-/-}$ stem cell exhaustion, a secondary transplantation experiment was carried out. Two to 3 primary recipients with similar GFP chimerism were killed at an average of 4 months after transplantation and BM cells were transplanted into 10 lethally irradiated (8 Gy) secondary recipients. Six of 10 recipients of *Runx1*$^{-/-}$ cells died within 3 months of secondary transplantation due to pancytopenia arising from graft failure, while all the recipients of control *Runx1*$^{+/+}$ cells survived

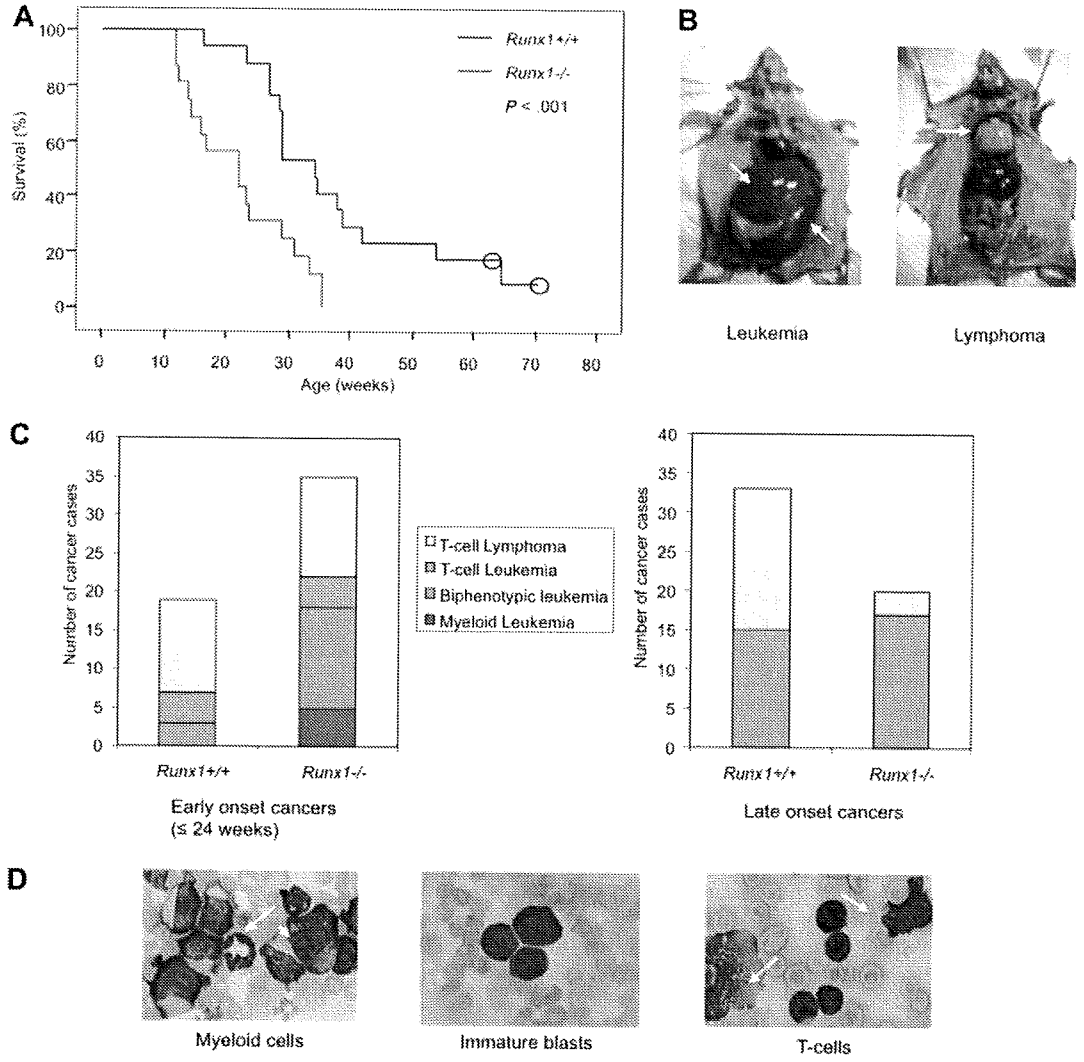

Figure 3. Runx1$^{-/-}$ mice show early onset and high frequency of leukemia with myeloid features in RIM. (A) Kaplan-Meier survival curves of *Runx1*$^{+/+}$ (blue line; n = 17) and *Runx1*$^{-/-}$ (red line; n = 16) mice injected with MoMuLV retrovirus. Kaplan-Meier method showed significant difference between the 2 genotypes ($P < .001$, Mantel-Cox test). Open circles represent censored cases. (B) Necropsy of diseased mice; leukemic mice usually show enlarged spleen (bottom arrow) and liver (top arrow) while T-cell lymphoma mice show enlarged thymus (arrow). (C) Graphs showing frequency of different types of leukemia/lymphoma, groups 1 to 4, in early-onset (≤ 24 weeks) cancers of *Runx1*$^{+/+}$ (n = 19) and *Runx1*$^{-/-}$ (n = 34) mice; and frequency of leukemia or lymphoma cases in late-onset cancers of *Runx1*$^{+/+}$ (n = 33) and *Runx1*$^{-/-}$ (n = 20) mice. In total, n = 52 for *Runx1*$^{+/+}$ mice and n = 54 for *Runx1*$^{-/-}$ mice. (D) Morphology of cells from PB of representative leukemic case from group 1 showing granulocyte (arrow) and monoblast (arrowhead); group 2 showing immature blasts; and group 3 showing T cells and ghost cells (arrows) which are frequently seen in T-cell malignancy.

beyond that (Figure 1D). Taken together, the above results prove that *Runx1*$^{-/-}$ status results in progressive stem cell exhaustion.

Surprisingly, colony assay of immature *Runx1*$^{-/-}$ cells (GFP$^+$ c-Kit$^+$Lineage$^-$) from BM of recipient mice showed an increased number of precursors even 2 years after transplantation, similar to the observations made soon after the conditional deletion of the *Runx1* gene[18] (Figure 2B). Furthermore, long-term culture initiating cell (LTC-IC) assay of KSL cells from BM of aged 40-week-old *Runx1*$^{-/-}$ mice showed an increased number of progenitor cells after 28 days of culture on OP9 stromal cells (Figure 2C). These results suggest that immature *Runx1*$^{-/-}$ cells maintain their inherent properties of increased proliferation even after long periods of time. Hence, stem cell exhaustion may not be due to cell intrinsic defects of *Runx1*$^{-/-}$ stem/progenitor cells.

Runx1$^{-/-}$ status results in increased susceptibility to myeloid leukemia development

It is conceivable that for *Runx1*$^{-/-}$ mice to develop leukemia, *Runx1*$^{-/-}$ stem cells would have to acquire an ability to survive long, possibly through additional genetic hits. Therefore, RIM was employed to induce leukemia in *Runx1*$^{-/-}$ mice and to identify genes that prevent stem cell exhaustion and aid in leukemia development. *Runx1*$^{-/-}$ mice showed a significantly shorter latency of leukemia development than wild-type littermates (Figure 3A), thus confirming that the Runx1-deficient status accelerates leukemia development.

When the mice became moribund, necropsy was carried out and the disease was divided into leukemia or lymphoma cases. Leukemia cases showed elevated leukocyte counts and hepatosplenomegaly with normal thymus, whereas lymphoma cases showed normal or elevated leukocyte counts and enlarged thymus/lymph node (Figure 3B). Based on combination of leukocyte counts, necropsy, and further immunophenotype and morphologic analyses, tumors were classified into the following 4 groups: group 1, myeloid leukemia (supplemental Figure 2A); group 2, biphenotypic (myeloid and T-cell) leukemia; group 3, T-cell leukemia; and group 4, T-cell lymphoma (supplemental Tables 1-2). Most of the biphenotypic leukemia cases belonging to group 2 were considered to be mixtures of myeloid and lymphoid leukemia originating from different clones, with a certain subset of the leukemic cells

Table 1. Classification of CISs identified in *Runx1*$^{+/+}$ and *Runx1*$^{-/-}$ mice

Classification of CIS/chromosome number*	Gene†	*Runx1*$^{+/+}$, n = 52	*Runx1*$^{-/-}$, n = 63
Known CISs, n = 16			
5	*Gfi1/Evi5*‡	2	11 (1)§, (3)‖
15	*c-Myc*‡	3	11
17	*Ccnd3*‡	2	6
7	*RRas2*	4	5
10	*Ahi1/Myb*	7 (1)¶	3 (2)#
2	*Rasgrp1*	2	2
11	*Ikaros***	1	2
3	*Evi1*‡	0	5
6	*Ccnd2*‡	0	3
12	*N-myc*‡,**	0	3
17	*Pim1*	0	3
2	*Bcas1*	0	2
5	*Bcl7a*	0	2
5	*Mad1l1***	0	2
7	*Sema4b*	0	2
12	*Jundm2*	0	2
Novel CIS, n = 4			
X	*Slis6*	0	4
3	*Slis7*	0	3
5	*Slis8*	0	2
16	*Slis9*	0	2

CIS indicates common integration site; and RIS, retroviral integration site.

*The genomic positions of the RIS were determined according to BLAT search of the UCSC Genome Bioinformatics database.

†Candidate genes in the vicinity of the RIS are shown.

‡CISs that are particularly interesting and are discussed in the text.

§Number in parentheses indicates number of integrations inside *Gfi1*.

‖Number in parentheses indicates number of integrations inside *Evi5*.

¶Number in parentheses indicates number of integrations inside *Myb*.

#Number in parentheses indicates number of integrations inside *Ahi1*.

**Genes with all retroviral integrations inside the gene.

expressing both the T-cell and myeloid markers simultaneously (supplemental Figure 2A).

In *Runx1*$^{-/-}$ mice, 34 of 54 (63.6%) developed early-onset (≤ 24 weeks) leukemia/lymphoma, whereas only 19 of 52 (36.5%) *Runx1*$^{+/+}$ mice showed early onset of leukemia/lymphoma. Out of the early-onset cases, 51.4% of *Runx1*$^{-/-}$ cases and 15.8% of *Runx1*$^{+/+}$ cases showed leukemia with myeloid features that fell into groups 1 and 2. The remaining mice developed T-cell leukemia/lymphoma that fell into groups 3 and 4 (Figure 3C). This result indicates that *Runx1* knockout status drives myeloid features in leukemias despite the strong T-lymphoid tropism of MoMuLV virus. Some of the group 1 and 2 leukemias recapitulated human RUNX leukemias with accumulation of immature blasts (as seen in AML M0) or accumulation of myeloid cells with differentiation (as seen in AML M2; Figure 3D).

Stemness related genes are preferentially affected in *Runx1*$^{-/-}$ leukemias

There were 710 retroviral integration sites (RISs) found in 63 *Runx1*$^{-/-}$ mice and 52 *Runx1*$^{+/+}$ mice. These sequences were mapped to the mouse genome to identify the chromosomal location of the sequences and to identify candidate genes at the loci. Twenty loci were affected more than once by retroviral integrations in *Runx1*$^{-/-}$ or *Runx1*$^{+/+}$ mice and these are referred to as common integration sites (CISs; Table 1). The relative locations of these integration sites were compared with the tags from the publicly available Retroviral-Tagged Cancer Gene Database.[27] This comparison revealed that 16 CISs correspond to previously known loci where retroviral integration occurred more than once. The other 4 CISs were detected only by our study and have been designated as Slis (Singapore leukemia integration site) and classified as novel CISs (Table 1, supplemental Table 3).

Genes near CISs that are affected with high frequency in *Runx1*$^{-/-}$ mice, but affected with lower frequency in *Runx1*$^{+/+}$ mice, may be specifically involved in leukemogenesis of *Runx1*$^{-/-}$ mice. Notably, candidate leukemogenic genes near CISs in Runx1-deficient leukemias with myeloid features are more relevant to our study since these leukemias recapitulate human RUNX1-related leukemias. A comprehensive list of genes (near CISs or RISs) that may be involved in tumor progression of each leukemia sample with myeloid features is given in Table 2. Interestingly, 10 of 18 *Runx1*$^{-/-}$ mice that developed leukemia with myeloid features had integrations near stem cell–related genes such as *Gfi1/Evi5*, *Evi1*, and *Lmo2*. These CISs are rarely affected in T-cell leukemia/lymphoma and preferentially hit in leukemia with myeloid features (supplemental Table 4).

Integrations at the *Gfi1/Evi5* locus, the locus where these 2 genes are located in the same direction in no overlapping fashion, were found in 11 of 63 *Runx1*$^{-/-}$ mice analyzed and only in 2 of 52 *Runx1*$^{+/+}$ mice ($P < .05$, Fisher test). Seven of the 11 *Runx1*$^{-/-}$ leukemia cases with integrations at the *Gfi1/Evi5* locus belonged to groups 1 and 2 (n = 18), which showed early-onset leukemia with myeloid features (Table 2). Gfi1 is a well-known factor involved in stem cell maintenance,[28] while Evi5 was recently shown to be a cell-cycle regulator that prevents premature entry of cells into mitosis.[29] Expression levels of *Gfi1* and *Evi5* were examined by qRT-PCR on cDNA from 6 of the available leukemic samples with integrations at this locus and 3 control samples without integration at this locus (Figure 4A). *Evi5* overexpression was seen in all affected *Runx1*$^{-/-}$ cases with integration outside this gene, and became pronounced as the distance between the RIS and the *Evi5* gene decreased. This indicates specific, integration site–dependent activation of *Evi5* expression. *Gfi1* expression was not significantly affected by viral integrations in majority of the cases (Figure 4B). Thus, *Evi5* overexpression appears to play a more cooperative role with Runx1 deficiency in leukemogenesis. Out of the integrations that were present only in *Runx1*$^{-/-}$ mice and not in *Runx1*$^{+/+}$ mice, the most frequent were integrations at the *Evi1* locus seen in 5 *Runx1*$^{-/-}$ mice, 3 of which belonged to groups 1 and 2 (Table 2). Evi1 functions in self-renewal, maintenance, and proliferation of stem cells.[30,31] Integrations near *c-Myc*, *Cyclin D2*, and *Cyclin D3* genes were also more frequent in *Runx1*$^{-/-}$ mice. *c-Myc* is a well-known protooncogene that causes uncontrolled proliferation of cells when overexpressed. *Cyclin D2* and *D3* are G_1 cyclins and their dysregulation leads to abnormal cycling of cells (Table 2).

Overexpression of *Evi5* cooperates with *Runx1*$^{-/-}$ status in long-term maintenance of aberrant stem/progenitor cells in vitro

To examine the details of cooperation with *Runx1*$^{-/-}$ status, *Gfi1*, *Evi5*, and *Evi1* were chosen from the RIM screen due to high frequency of viral integrations near these genes in *Runx1*$^{-/-}$ leukemias compared with wild-type cases. We deduced that they are likely to prevent exhaustion of *Runx1*$^{-/-}$ stem cells due to their possible function in stem cell maintenance and thus contribute to development of Runx1-related leukemia.

To study the effect of overexpression of these candidate oncogenes in immature hematopoietic cells, the c-Kit$^+$ fraction of BM cells transfected with MIG vector carrying *GFI*, *EVI5*, or *EVI1*

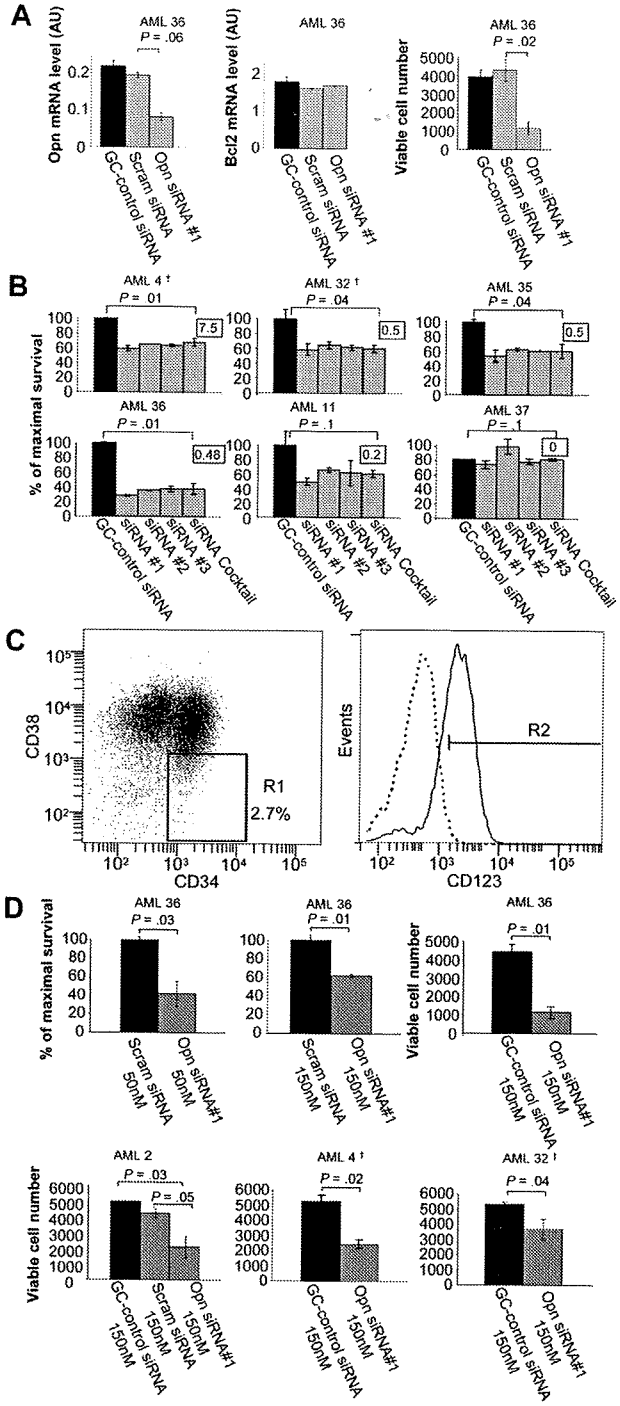

Figure 6. siRNA-mediated knockdown of *OPN* expression reduces cell survival in AML blasts and LSPCs. Purified CD34$^+$ cells from the indicated AML patient samples were transfected with 50nM BLOCK-iT fluorescent oligo and 50 to 150nM of (1) RNAi High GC negative control duplexes; (2) scrambled siRNA duplexes; (3) *OPN* siRNAs duplexes no. 1, no. 2, or no. 3; or (4) a cocktail consisting of all 3 *OPN* siRNAs duplexes (A-B,D). After transfection, cells were cultured for 2 to 3 days in IMDM medium containing 0.5% FCS, after which time total RNA was isolated for quantitative RT-PCR (A) and viable cell number was assessed by using Flow-Count Fluorospheres (A,D). (B) Cell survival was determined by annexin V–Alexa 568 staining and flow cytometry. The survival of purified CD34$^+$ cells isolated from patients with AML in culture varied from 15% to 90%, and results are presented as the percentage of cell survival relative to the control siRNA-transfected cells. The inset indicates the level of *OPN* mRNA expression for each AML sample as determined in Figures 4 and 7. (C) AML CD34$^+$/CD38$^-$/CD123$^+$ LSPCs were purified by fluorescence-activated cell sorting (FACS). Cells were stained with CD34-FITC, CD38-PE-Cy7, and CD123-PE antibodies after which time LSPCs were sorted with FACSAria cell sorter into CD34$^+$CD38$^-$ subpopulation (1%-2% of total live cells) and gated for high CD123 expression (0.5%-1% of total). Approximately 5×10^5 to 1×10^6 cells were obtained from a single sort of 2×10^8 thawed cells. The purity of sorted populations was confirmed by secondary flow cytometry. (D) LSPCs were transfected and analyzed for cell survival as described in panel A. †Samples were derived from relapsed patients.

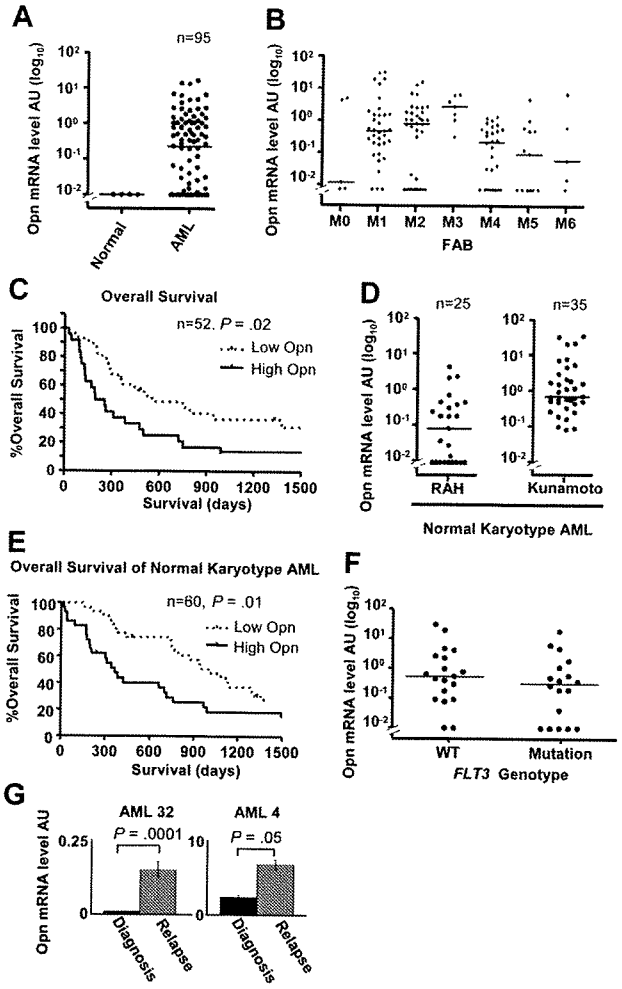

Figure 7. Increased *OPN* expression is associated with poor OS in AML. (A) Scatterplot showing *OPN* expression determined by quantitative RT-PCR in 4 normal CD14$^+$ monocyte controls and 95 diagnostic samples from consecutive patients with AML collected at the RAH of which 60 were treated with induction chemotherapy. The horizontal lines indicate the median expression of *OPN* (0.23 AU). (B) Scatterplot of the range and median of *OPN* expression for various FAB classifications for all patients analyzed (95 RAH plus 35 Kunamoto normal karyotype patients). There is a significant difference in median *OPN* expression between FAB M3 and M4 or M5 subgroups ($P = 0.01$, Kruskal-Wallis test; $P < .05$, Dunn multiple comparisons test). (C) Kaplan-Meier log-rank analysis of all patients from RAH who underwent standard induction chemotherapy, excluding acute promyelocytic leukemia (APML; M3; n = 52). Taking a cutoff of 0.23 AU (median; split panel A), patients were divided into either high *OPN* expressers (> 0.23 AU) or low *OPN* expressers (< 0.23 AU). (D) Scatterplot showing the range and median of *OPN* expression for cytogenetically normal AML patient samples obtained at RAH (n = 25) and Kunamoto (n = 35), which were analyzed for OS (E). (E) Kaplan-Meier survival curves for the combined patients with normal cytogenetic AML shown in panel D after standard induction chemotherapy (n = 60), comparing high versus low *OPN* expression as determined by median split of each cohort as shown in panel D. High *OPN* is associated with poor OS (median, 384 days) compared with low *OPN* (median, 1017 days; $P = .01$). (F) Scatterplot comparing *OPN* expression in patients with cytogenetically normal AML analyzed in panel E for which *FLT3* mutation status had been determined (ITD or D835 mutation; n = 37). There was no difference in median *OPN* expression between the 2 groups (n = 37; $P = .2$, Mann-Whitney *U* test). (G) Two patients for whom cryopreserved diagnosis and relapse samples were available were examined for *OPN* expression by quantitative RT-PCR. A significant increase in *OPN* expression was observed in both patients at relapse ($P < .05$, Mann-Whitney *U* test).

associated with higher mean age (52 vs 42 years; $P = .02$, Student *t* test) and increased M1 FAB classification (53% vs 23%; $P = .01$, χ^2 test; supplemental Table 4). Importantly, our results show that patients with high *OPN* expression had a significantly shorter OS (median, 384 days) compared with patients with low *OPN* expression (median, 1017 days; Figure 7E; n = 60; HR, 2.05; 95% CI,

Table 1. Characteristics of the 52 consecutive patients treated with induction chemotherapy according to *OPN* status

	Total patients, n = 52	OPN high, n = 25 (48%)	OPN low, n = 27 (52 %)	*P*
Median *OPN* level (range)	0.20 (0.00-13.1)	0.775 (0.23-13.7)	0.00 (0.00-0.20)	N/A
Mean age, y, mean ± SD	51 ± 17	55 ± 15	48 ± 18	.2
Male, n (%)	29 (55)	15 (60)	14 (51)	.7
Median WBC count, $\times 10^9$/L (range)	11.9 (1.3-300)	15.9 (1.3-300)	7 (1.68-171)	.7
Median BM blasts, % (range)	67 (20-99)	55 (22-92)	70 (20-99)	.8
FAB, n (%)				
M0	2 (4)	1 (4)	1 (4)	N/A
M1	19 (36)	10 (40)	9 (33)	N/A
M2	14 (26)	8 (32)	6 (22)	N/A
M4	7 (13)	2 (8)	5 (18)	N/A
M5	7 (13)	3 (12)	4 (15)	N/A
M6	2 (7)	1 (4)	2 (7)	.9
Cytogenetic subgroup, n (%)				
Unfavorable	11 (21)	7 (28)	4 (14)	N/A
Intermediate	37 (71)	15 (60)	22 (81)	N/A
Favorable	3 (6)	3 (12)	0 (0)	.07
FLT3 mutation, n (%)	14/20 (70)	5/8 (63)	9/12 (75)	.6
Induction chemotherapy, n (%)	52 (100)	25 (100)	27 (100)	< .99
Allotransplantation, n (%)	11/52 (21)	4/25 (16)	7/27 (25)	.5

All patients were treated with standard AML induction therapy that included cytarabine, idarubicin, and etoposide followed by consolidation chemotherapy. Patients with APML(M3) treated with *all-trans* retinoic acid–based regimens were excluded. The mean age of our cohort was 51 years with a median follow-up of living patients at 5 years. The 5-year OS rate was 23%. FLT3 mutation status (internal tandem duplication of FLT3 receptor or D835 point mutation) was available for 20 patients (38%). Differences in the distribution of patients between FAB subgroups and cytogenetic risk groups were tested for categorical variables by χ^2 test. Differences in continuous variables were tested with the Student *t* test or Mann-Whitney *U* test when appropriate.

WBC indicates white blood cell; N/A, not applicable; and cytogenetic subgroups, karyotype risk groups were defined according to the MRC10 criteria.

1.20-3.88; $P = .01$), suggesting that high *OPN* may be associated with inferior outcome in normal karyotype AML. In those patients for which *FLT3* status had been determined, there was no significant association between *OPN* expression and the presence of a *FLT3* mutation ($P > .05$, Mann-Whitney *U* test; Figure 7F). The prognostic effect of *OPN* in normal cytogenetic AML was further investigated by a multivariate Cox proportional hazards model that included age, WCC, and treatment center. Only age and *OPN* remained significant at a *P* value less than .05 (Table 3). When we controlled for these factors, *OPN* remained significantly associated with poor OS (n = 60; HR, 2.22; 95% CI, 1.23-4.02; $P = .01$), suggesting that high *OPN* expression is an independent prognostic indicator in normal karyotype AML (Table 3).

Because *OPN* expression was associated with poor OS, we considered the possibility that *OPN* expression may be increased in relapsed patient samples. We therefore compared *OPN* expression in 2 patients for whom both diagnostic and relapsed cryopreserved AML samples were available. Analysis of both these samples showed that *OPN* mRNA expression levels were significantly increased after disease relapse (Figure 7G; $P < .05$), further supporting the findings (Figure 7A-E) that high *OPN* expression is a prognostic indicator linked to inferior patient outcome and early death after chemotherapy.

Table 2. Multivariate analysis of the prognostic effect of *OPN* and other prognostic variables on overall survival

Prognostic marker	Level	Hazard ratio	95% CI	*P*
OPN	High	1.79	0.94-3.39	.08
Age	Continuous	1.02	0.99-1.05	.06
WCC	Continuous	1.006	1.001-1.012	.02
Cytogenetics				.03*
	High	3.71	0.91-15.08	.07
	Intermediate	1.26	0.37-4.32	.7
	Low	1.0	—	—

The effect of *OPN* expression on overall survival for 52 patients with AML treated with chemotherapy in our institution was examined in a multivariate Cox proportional hazards model that included all variables that were deemed influential in survival: *OPN*, age, white cell count (WCC) at diagnosis, and cytogenetic risk group. The assumptions for proportional hazards was not violated.

— indicates not applicable.

*Global *P* value for cytogenetics.

Discussion

Deregulated cell survival is a classic hallmark of cancer and therefore represents a key therapeutic target.[28] We now show that Ser585-survival signaling regulates a transcriptional program comprising multiple gene networks (Figure 1), including a pathway that regulates *OPN* and a set of targets of the PI3-kinase pathway with established roles in cancer and cell death (Figure 3). We further show that Ser585 signaling is deregulated in the majority of AML patient samples (20 of 23) representing diverse FAB and cytogenetic classifications (Figure 4). In contrast, no deregulation of Tyr577 phosphorylation was observed in most of the AML patient

Table 3. Multivariate analysis of the prognostic effect of *OPN* in normal karyotype AML on OS

Prognostic marker	Level	Hazard ratio	95% CI	*P*
OPN	High	2.226	1.231-4.027	.01
Age	Continuous	1.028	1.007-1.050	.01
WCC	Continuous	1.002	1.000-1.004	.07

The effect of *OPN* expression on OS of 60 consecutive patients with normal cytogenetics treated with induction chemotherapy was examined in a multivariate Cox proportional hazards model that included age, WCC, and treatment center as potentially influential variables. After controlling for age and WCC, high *OPN* expression (high vs low) remained a significant predictive factor for OS ($P = .01$). Treatment center was not influential on prognosis after multivariate analysis ($P = .9$; data not shown), and there was no significant interaction between *OPN* and other prognostic variables at each treatment center. The assumptions for proportional hazards was not violated.